Accepted Manuscript

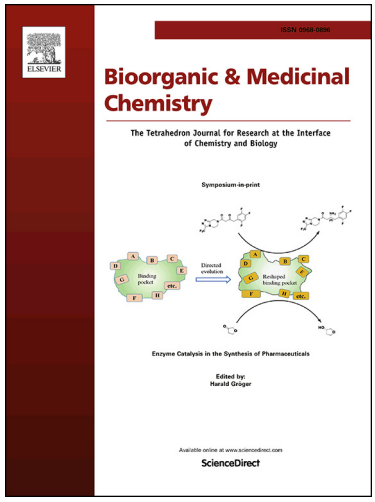

Synthesis and biological properties of aryl methyl sulfones

Lorena Navarro, Gloria Rosell, Silvia Sánchez, Núria Boixareu, Klaus Pors, Ramon Pouplana, Josep M. Campanera, M. Dolors Pujol

PII: S0968-0896(18)30914-3
DOI: https://doi.org/10.1016/j.bmc.2018.06.038
Reference: BMC 14430

To appear in: *Bioorganic & Medicinal Chemistry*

Received Date: 11 May 2018
Revised Date: 26 June 2018
Accepted Date: 28 June 2018

Please cite this article as: Navarro, L., Rosell, G., Sánchez, S., Boixareu, N., Pors, K., Pouplana, R., Campanera, J.M., Pujol, M.D., Synthesis and biological properties of aryl methyl sulfones, *Bioorganic & Medicinal Chemistry* (2018), doi: https://doi.org/10.1016/j.bmc.2018.06.038

Synthesis and biological properties of aryl methyl sulfones

Lorena Navarro,[‡] Gloria Rosell,[‡] Silvia Sánchez,[¥] Núria Boixareu,[€] Klaus Pors,[€] Ramon Pouplana,[§] Josep M. Campanera,[§]* and M. Dolors Pujol[‡]*

[‡]*Laboratori de Química Farmacèutica (Unitat Associada al CSIC). Facultat de Farmàcia. Universitat de Barcelona. Av. Diagonal 643. E-08028-Barcelona (Spain)*

[§] *Departament de Farmàcia i Tecnologia Farmacèutica, i Fisicoquímica, Facultat de Farmàcia i Ciències de l'Alimentació, Universitat de Barcelona, Av. Diagonal 643, E-08028, Barcelona (Catalonia, Spain)*

[¥]Unitat de Farmacologia, Departament Patologiai Terapèutica Experimental. Facultat de Medicina. Universitat de Barcelona. L'Hospitalet de Llobregat. E-08907-Barcelona (Spain)

[€]Institute of Cancer Therapeutics, School of Pharmacy and Medical Sciences, Faculty of Life Sciences, University of Bradford, BD7 1DP, West Yorkshire, U.K.

*To whom correspondence should be addressed. For M.D.P.: E-mail: mdpujol@ub.edu, phone, +34-93-4024534; fax, +34-93-4035941. [a]Abbreviations: COX-1, cyclooxigenase-1; COX-2, cyclooxigenase-2; NSAIDs, Nonsteroidal anti-inflammatory drugs; PG, prostaglandin; PGH_2, prostaglandin G_2; SAR, structure-activity relation-ships; QSAR, quantitative structure-activity relation-ships.

ABSTRACT: A novel group of aryl methyl sulfones based on nonsteroidal anti-inflammatory compounds exhibiting a methyl sulfone instead of the acetic or propionic acid group was designed, synthesized and evaluated *in vitro* for inhibition against the human cyclooxygenase of COX-1 and COX-2 isoenzymes and *in vivo* for anti-inflammatory activity using the carrageenan induced rat paw edema model in rats. Also, *in vitro* chemosensitivity and *in vivo* analgesic and intestinal side effects were determined for defining the therapeutic and safety profile. Molecular modeling assisted the design of compounds and the interpretation of the experimental results. Biological assay results showed that methyl sulfone compounds **2** and **7** were the most potent COX inhibitors of this series and best than the corresponding carboxylic acids (methyl sulfone **2**:

IC_{50} COX-1 = 0.04 and COX-2 = 0.10 μM, and naproxen: IC_{50} COX-1 = 11.3 and COX-2 = 3.36 μM). Interestingly, the inhibitory activity of compound **2** represents a significant improvement compared to that of the parent carboxylic compound, naproxen. Further support to the results were gained by the docking studies which suggested the ability of compound **2** and **7** to bind into COX enzyme with low binding free energies.

The improvement of the activity of some sulfones compared to the carboxylic analogues would be performed through a change of the binding mode or mechanism compared to the standard binding mode displayed by ibuprofen, as disclosed by molecular modeling studies. So, this study paves the way for further attention in investigating the participation of these new compounds in the pain inhibitory mechanisms. The most promising compounds **2** and **7** possess a therapeutical profile that enables their chemical scaffolds to be utilized for development of new NSAIDs.

Keywords: anti-inflammatory, analgesic, NSAIDs, methyl sulfones, COX-inhibitors, binding free energy estimation

1. Introduction

Non-steroidal anti-inflammatory drugs (NSAIDs) are the most prescribed pharmaceutical compounds in the world to alleviate inflammation and pains associated with several pathological conditions and are often the initial treatment for common inflammation. NSAIDs are a heterogeneous group of various chemical structures with variable benefit/risk profile. Usually the use of NSAIDs is associated with several adverse effects, including gastrointestinal damage. The clinically used NSAIDs exert their therapeutical effects by inhibition of the biosynthesis of prostaglandins (PGs) and thromboxanes (TX). In general, the biosynthesis involves the conversion of arachidonic acid to prostaglandin G_2 (PGH_2), a reaction catalyzed by the sequential action of cyclooxygenase (COX) (Figure 1). Most NSAIDs inhibit COX-1 and COX-2

isoforms.[1,3] The constitutive COX-1 is responsible for the synthesis of cytoprotective prostaglandins in the gastrointestinal tract, and for the pro-aggregator thromboxane in blood platelets.[4] In the inflammation process COX-2 is responsible for production of prostaglandins, considered mediators of inflammation (Figure 1).

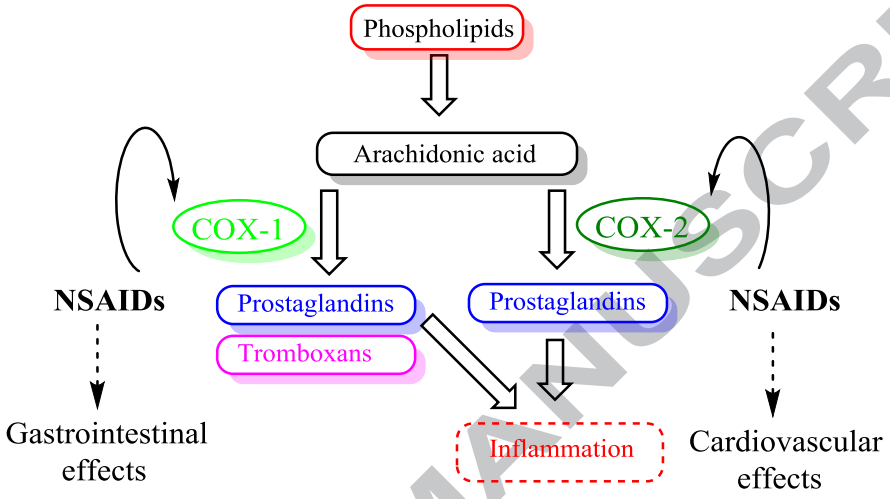

Figure 1. Inflammation biochemical pathways

It has recently been reported that classical NSAIDs such as celecoxib possess preventive effects against colorectal cancer (CRC)[5] and Alzheimer's disease.[6] Moreover, these compounds continue to be used as remedies for rheumatic[7] and autoimmune anti-inflammatory diseases.[7c] In general, NSAIDs (Figure 2) are potent anti-oxidants that exert both anti-inflammatory and antitumor activity.[8-10] In regard the latter, ibuprofen inhibits tumor growth and liver metastasis.[9a] While long-term use of acetaminophen enhances the development of leukemia regular treatment with NSAIDs correlates with a reduced risk of lymphoma and leukemia development.[11] The chronic use of NSAIDs inhibit the growth of adenomatous polyps of patients with familial adenomatous polyposis and reduce the risk of CRC.[12] Selective COX-2 inhibitors showed a safe profile in the gastrointestinal tract, but recent studies suggest that the long-term treatment by selective COX-2 inhibitors is limited because of cardiovascular thrombotic events related to the

aggregatory properties of these drugs.[13] Moreover, COX-2 makes a significant contribution to the production of inflammatory PGs while the inhibition of COX-2 attenuates the expression of inflammatory mediators such as TNF-α, iNOS and IL-1β.[14] NSAID compounds are often associated with the presence of gastrointestinal side effects and new agents with diminished off-target effects are highly desirable.

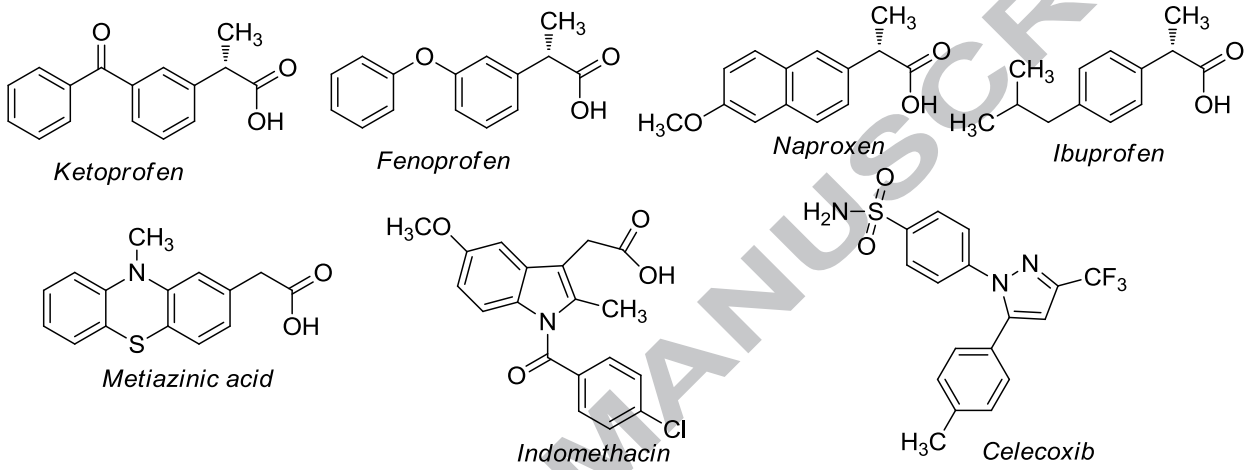

Figure 2. Classical NSAIDs

In the present study based on the previous work[15] related to COX-1/COX-2 inhibitors and the properties of NSAIDs, we designed a series of seven new compounds derived from classic and commercial NSAIDs in order to study their potential therapeutic properties (Figure 3). Specifically, the purpose of the study was to evaluate whether the replacement of the acetic or propionic acid group by a methyl sulfone group, a more lipophilic group with low acidic properties, could lead to high COX activity and reduced risk of side-effects, thereby result in better anti-inflammatory and safety profile than the parent classical NSAIDs scaffolds.

Here we report on the synthesis of a series of sulfones as a new class of NSAIDs and report on their biological properties by comparing them with the respective carboxylic acids chosen as models.

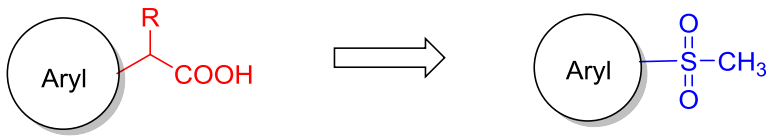

Fenoprofen (arylpropionic acid, R = CH_3)
Naproxen (arylpropionic acid, R = CH_3)
Ibuprofen (arylpropionic aci, R = CH_3)
Metiazinic acid (arylacetic acid, R = H)
Indomethacin (arylacetic acid, R = H)

Ketoprofen (arylpropionic acid, R = CH_3)
Ketoprofen (arylpropionic acid, R = CH_3)

1. Aryl = 3-(phenoxy)phenyl
2. Aryl = 2-(6-methoxynaphthalenyl)
3. Aryl = 4-(isobutylphenyl)
4. Aryl = 10-methyl-phenothiazyn-2-yl
5. Aryl = 3-(2-methyl-5-methoxy-1-(4-chlorophenylcarbonyl)indolyl)
6. Aryl = 4-(4-chlorophenylcarbonyl)phenyl
7. Aryl = 4-(3-furanylcarbonyl)phenyl

Figure 3. Design strategy of methyl sulfones

Compounds **1-5** derive from the direct substitution of alkylcarboxylic group by methyl sulfone of the classical NSAIDs fenoprofen, naproxen, ibuprofen, metiazinic acid and indomethacin respectively, and were chosen due to their structural variability and anti-inflammatory profile. Two additional methyl sulfones were also studied, compounds **6** and **7**, which were derived from not only a direct substitution of the alkyl carboxylic acid of ketoprofen but also changes at other positions of the scaffold.

2. Results and discussion

2.1. Synthesis and biological evaluation of methyl sulfones

The methods used for the synthesis of aryl sulfones from different starting materials were readily available and enabled the synthesis of target compounds in a conventional and safe manner. The general synthetic routes are illustrated in Schemes 1-7.

The methyl sulfone **1** was prepared from 1-bromo-3-methylsulfonylbenzene (**9**) and phenol under cross-coupling conditions,[16] which was obtained from 3-bromothioanisole (**8**) by oxidation with *m*-CPBA (Scheme 1).

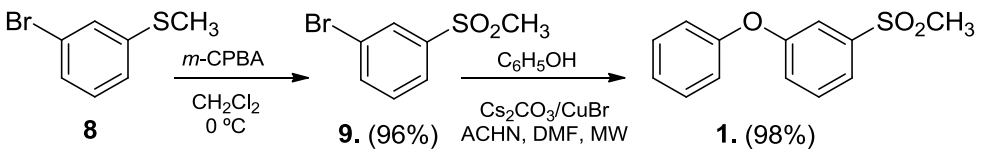

Scheme 1. Synthesis of compound **1**

2-Bromo-6-methoxynaphthalene (**10)** was transformed to the methylthionaphthalene derivative **11** using butyl lithium for the Br/Li interchange, followed by addition of dimethyl disulfide (DMDS). Methyl sulfone **2** was obtained by oxidation of **11** with *m*-CPBA (Scheme 2).

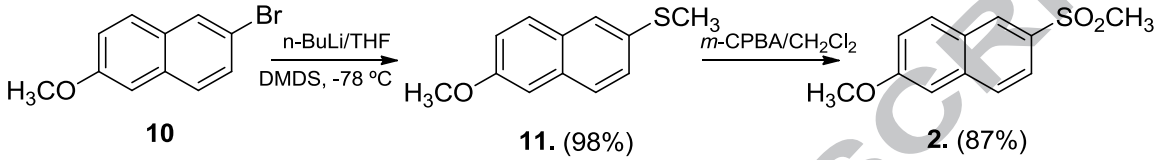

Scheme 2. Synthesis of compound **2**

The methyl sulfone **3** was obtained in a three-step procedure: thioanisole was subjected to Friedel Crafts acylation, followed by oxidation of the methylthio intermediate **14** to the corresponding methyl sulfone **15** with *m*-CPBA using the optimized conditions described above (Scheme 3). The final step involved Clemmensen conditions using Zn-$HgCl_2$ to obtain target compound **3**.[17]

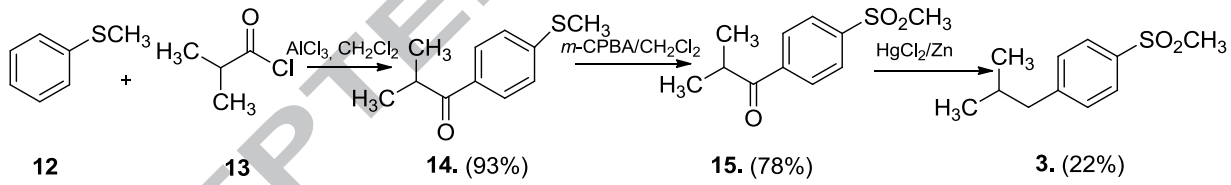

Scheme 3. Synthesis of compound **3**

The phenothiazine **4** was prepared in 3-step transformation from the commercial phenothiazine **16** (Scheme 4). *N*-Acylation of the phenothiazine under classical conditions followed by methylsulfonation at the C-2 position and later alkylation with methyl iodide at the position 10 of the heterocycle led to the desired methyl sulfone in acceptable overall yield (19%).

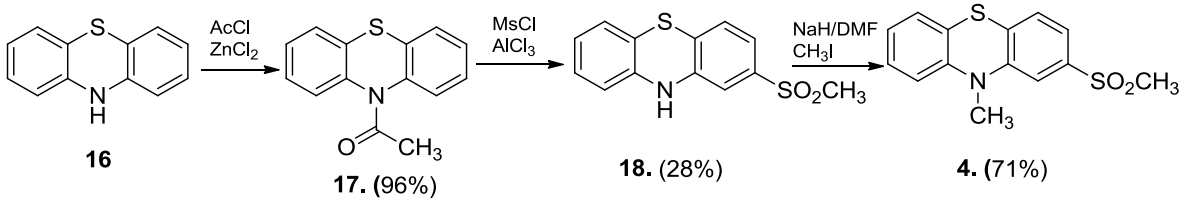

Scheme 4. Synthesis of compound **4**

The 3-iodoindole **20** was prepared by iodination of the commercial indole **19** using molecular iodine and potassium hydroxide to afford the resulting 3-iodoindole **20**, which was converted into methylmercaptane **21** with dimethyldisulfide (DMDS) via a lithium intermediate in excellent yields. Then regioselective oxidation of **21** with *m*-CPBA provided the methyl sulfone **22**, which was reacted with 4-chlorobenzoyl chloride in DMF to afford the *N*-acylated target compound **5** (Scheme 5).

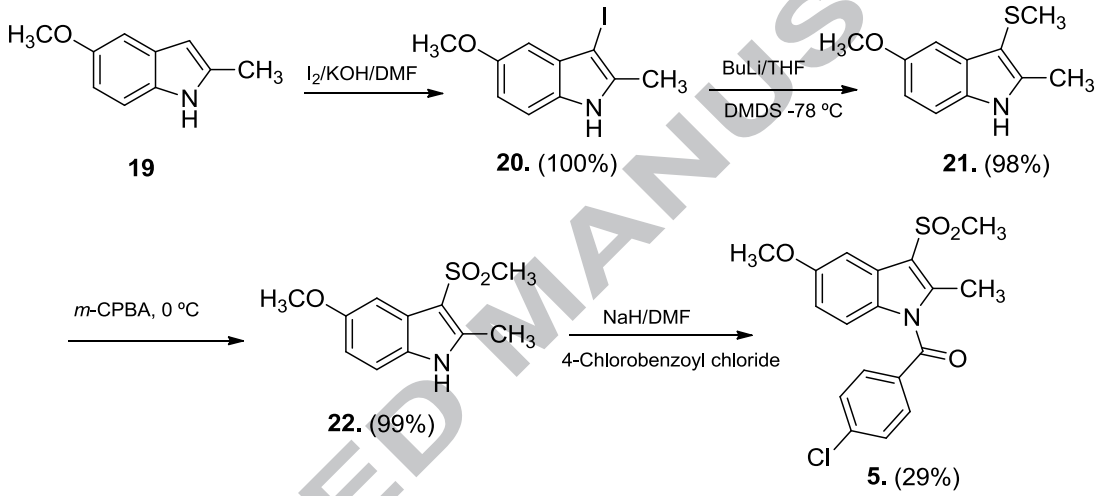

Scheme 5. Synthesis of compound **5**

The methyl sulfone **6** was prepared by oxidation of the methylthio derivative to the corresponding sulfone using *m*-CPBA[18] (Scheme 6). The intermediate benzophenone (**24**) was obtained in one step by acylation of commercial thioanisole (**12**) with 4-chlorobenzoyl chloride (**23**) under classical conditions.

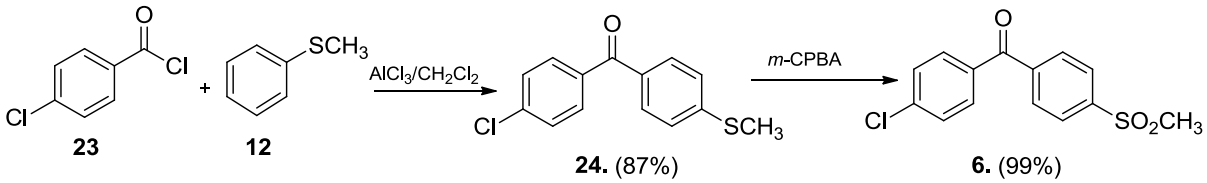

Scheme 6. Synthesis of compound **6**

Thioanisole **12** was reacted with furan-3-yl carboxylic acid chloride under Friedel Crafts conditions using $TiCl_4$ as a catalyst. The resulting ketone **26** was oxidized with *m*-CPBA to afford the methyl sulfone **7** in high yield (Scheme 7).

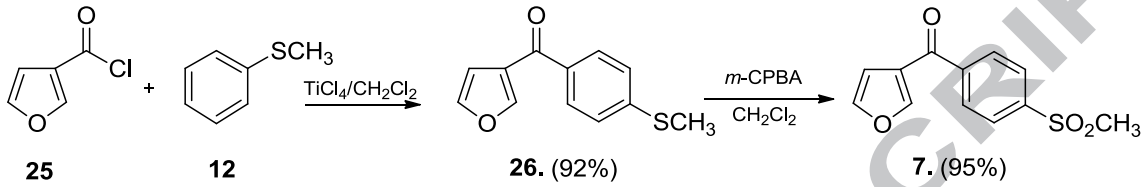

Scheme 7. Synthesis of compound **7**

2.2. Pharmcology

Biological Results. Synthesized methyl sulfones **1-7** were assayed *in vitro* cyclooxygenase inhibition, *in vivo* anti-inflammatory activity, *in vivo* analgesic activity, *in vivo* gastrointestinal side effects and the chemosensitivity in human cells.

***In Vitro* Cyclooxygenase 1 and Cyclooxygenase 2 Inhibition.** The methyl sulfones and the reference compounds were tested at the same concentrations (10 μM, 1 μM, and 1 nM).

In vitro COX-1/COX-2 isoenzyme inhibition studies [19] showed that compounds **2**, **3**, **5**, **6** and **7** were more potent inhibitors of COX-1 compared with COX-2 (Table 1) while **1** was shown to be slightly more selective for COX-2 (Table 1, entry 3). Compounds **1**, **2** and **5** exhibited a prominent COX inhibition (IC_{50} < 1 μM, Table 1, entries 1, 3 and 11). Moreover, compounds **1** and **2** are the only methyl sulfones of these series that improve the potency of COX-2 inhibition in regard to their carboxylate analogues by 93- and 33- fold, respectively. The methyl sulfone **5** was equipotent and non-selective to its carboxylate analogue, indomethacin (Table 1, entries 10 and 11).

Compound **6** was less potent than ketoprofen when measured against both COX-1 and COX-2 isoenzymes. Also the methyl sulfone **3** showed less activity than the parent NSAIDs ibuprofen. In contrast, sulfone **1** was equipotent with fenoprofen in regard to COX-1 but almost 100-fold more superior against COX-2. Methyl sulfones **2** and **7** showed interesting inhibitory COX-1 and COX-2 activities but little differential isoform selectivity. The phenothiazine **4** presents an inhibiting activity against COX-1 (4.5-fold) and COX-2 (5.8-fold) and is superior to the metiazinic acid. The pyrrole **7** was designed according to the molecular modelling results of the different interactions between several NSAIDs drugs and COX-1 and COX-2 isoforms and it is related to ketoprofen. Compound **2**, an analogue of naproxen, was the most active novel compound with COX-1 and COX-2 inhibitory activity higher than any of the known NSAIDs in this study apart from inhibition of COX-2 by celecoxib.

Only the methyl sulfone **1** was shown to be selective for COX-2 compared to COX-1 with an activity ratio of 17.5 (table 1, entry 13); this observation might be important as **1** could exhibit relatively low propensity for causing gastric damage.

Table 1. *In vitro* Anti-inflammatory Activity

Entry	Compound	COX-1 (μM) IC_{50}	COX-2 (μM) IC_{50}	Selectivity COX-2 (COX-1/COX-2)
1	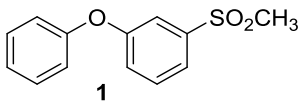 **1**	4.89±0.97	0.28±0.05	17.47
2	***Fenoprofen****	2.73±0.44	26.3±1.67	0.10
3	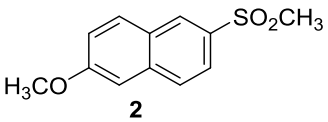 **2**	0.04±0.001	0.10±0.02	0.4
4	***Naproxen****	11.30±1.08	3.36±0.87	3.36

5	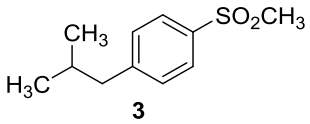 **3**	7.02±0.88	22.04±1.23	0.32
6	***Ibuprofen***[15]	3.20	1.50	2.10
7	***Ibuprofen****	3.35±0.94	1.40±076	2.40
8	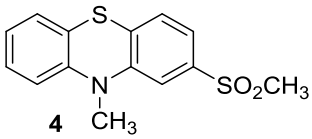 **4**	1.36±0.12	1.79±0.09	0.76
9	***Metiazinic acid****	6.23±0.85	10.45±1.10	0.60
10	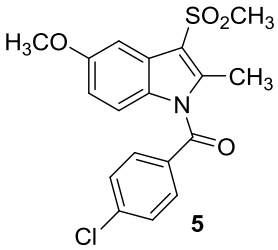 **5**	0.39±0.01	0.76±0.02	0.51
11	***Indomethacin****	0.10±0.05	0.90±0.12	0.11
12	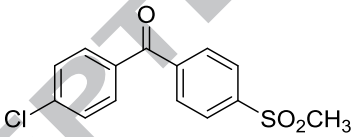 **6**	5.29±0.78	11.37±1.02	0.47
13	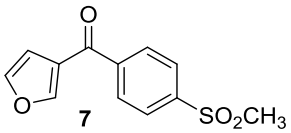 **7**	0.18±0.07	0.71±0.12	0.25
14	***Ketoprofen****	0.11±0.09	0.18±0.07	0.61
15	***Celecoxib***[20]	22.90	0.0507	404
16	***Celecoxib***[15]	6.86	0.10	69
17	***Celecoxib****	7.10±0.79	0.11±0.02	65

Results are expressed as the mean (n = 3) of the % inhibition of PGH_2 production by test compounds with respect to control samples. *In vitro* COX-2 selectivity index (IC_{50}COX-1 /IC_{50} COX-2). *Test *in vitro* realized by us in this work.

The comparison of COX-2 binding affinities of methyl sulfones versus carboxylic compounds revealed that five compounds, **1**, **2**, **4**, **5** and **7**, exhibit an improvement in the binding affinity (Figure 4). However the most surprising result may be the high inhibition of COX-1 showed by sulfone **2**, which was considered the most active of this series. The above-mentioned compound has a 283-fold higher activity against COX-1 and 34 against COX-2 than naproxen (the parent compound) and also a higher activity than any of the NSAIDs in this study apart from ketoprofen and celecoxib (Figure 4). Furthermore, the pyrrole derivative **7** showed major activity against COX-1 (63 times) and COX-2 (5 times) than the reference naproxen.

In general, for methyl sulfones, the more rigid compounds have a better anti-inflammatory activity than the more flexible ones (Table 1, compounds **2**, **4** and **5** versus **1**, **3** and **6**), while in arylacetic and arylpropionic acids it is not so clear (Table 1, entries 4, 9 and 11).

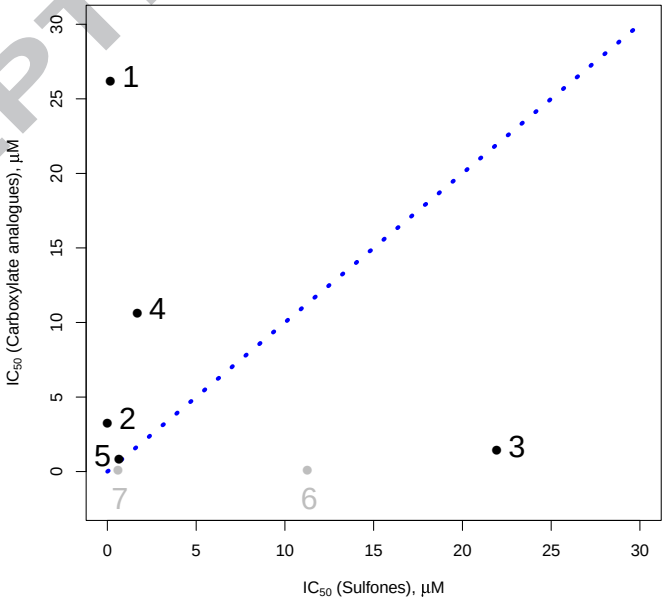

Figure 4. Experimental COX-2 binding affinities (IC_{50}) of the sulfones derivatives compared to carboxylate analogues. Sulfone derivatives below the dotted line (in blue) are less active than the corresponding carboxylate analogues whereas the compounds located upper the dotted line behave oppositely. Compounds that derive from the substitution of the arylacetic or arylpropionic acid group by a methyl sulfone group in a classical NSAID are colored

in black (compounds **1**-**5**), whereas in grey those sulfone compounds that indirectly derive from ketoprofen (compounds **6** and **7**). As can be seen, compound **2** is the most active.

***In Vivo* Anti-inflammatory Activity.** The % inhibition of inflammation oral dose was determined using a carrageenan induced paw edema protocol in rats and the ibuprofen was used as a reference compound for the *in vivo* assays.[21] These compounds were tested to reduce the formation of edema in a dose of 70 mg/Kg and time-dependent manner. The edema volume was determined at 3 and 4 h after the carrageenan injection. Compounds **3** and **6**, analogues of ibuprofen and ketoprofen, respectively showed low anti-inflammatory activity (Table 2, entries 3 and 6) attributable to problems of solubility very marked for the sulfone **3** analog of ibuprofen. Compounds **1**, **2**, **5** and **7** reduced inflammation between 27.8 and 29.9% at 3 h post-carrageenan and 25.4 to 34.6% after 4 h. The naproxen analogue **2** and the indomethacin derivative **5** displayed an interesting anti-inflammatory profile, showing 29.4 and 29.9% inhibition by the 3 h but reached 34.6 and 32.5% inhibition of inflammation at 4 h after carrageenan respectively. Both compounds demonstrated inhibition of the carrageenan paw edema with sustained activity after 4 h, which was markedly better than ibuprofen.

Table 2. *In vivo* Anti-inflammatory Activity

		3 h		4 h	
Entry	Compound	swelling	% inhibition	Swelling	% inhibition
1	**1**	a) 28.1 ± 2.5**	27.8	a) 34.0 ± 3.9**	25.4
		b) 38.9 ± 6		b) 45.6±6.3	
2	**2**	a) 33.1 ± 3.6 ***	29.4	a) 35.2 ± 3.5***	34.6
		b) 46.9 ± 3.6		b) 53.8 ±3.6	
3	**3**	a) 32.3 ± 2.8 **	9.6	a) 38.4 ± 3.2 *	9.5
		b) 35.7 ± 6.9		b) 42.5 ± 5.2	
4	**4**	a) 39.6 ± 5.3 #	NA	a) 45.6 ± 6.3	NA

		b) 38.9 ± 6		b) 44.8 ± 5.4	
5	**5**	a) 32.9 ± 4.1 ***	29.9	a) 36.3 ± 5.1***	32.5
		b) 46.9 ± 3.6		b) 53.8 ± 3.6	
6	**6**	a) 43.2 ± 4.8 *	14.9	a) 50.0 ± 5.3*	18.9
		b) 50.7 ± 5.5		b) 61.7 ± 6.4	
7	**7**	a) 36.7 ± 6.2**	27.6	a) 45.7 ± 4.5**	25.9
		b) 50.7 ± 5.5		b) 61.7 ± 6.4	
8	***Ibuprofen***	a) 27.1 ± 3.6***	30.3	a) 34.4 ± 6.9 **	23.9
		b) 38.9 ± 6.0		b) 45.1 ± 5.0	

a) Swelling for the dose of 70 mg/Kg. b) Swelling control. NA no activity attributable due to low solubility in water.
Values significantly differ from controls as indicated: *P<0.05; **P<0.01; ***P<0.001; # does not differ significantly according to unpaired one-tailed Student's *t*-test.
The data represent the mean ±S.E.M. of 6 animals (p<0.05). The rat paw edema occurred at 3 and 4 h post-carrageenan administration.

The methoxynaphthalen of naproxen and the *N*-acylindole of indomethacin (compounds **2** and **5**) confer greater activity both *in vitro* and *in vivo* than the substituted phenyl groups of fenoprofen, ibuprofen or ketoprofen (compounds **1**, **3** and **6**). Compound **7** containing the pyrrole ring showed high activity, much more *in vivo* than *in vitro* but inferior to naproxen. The *in vivo* anti-inflammatory activity of the phenothiazine **4** could not be determined due to problems of poor solubility in water.

Analgesic Activity

In general, analgesic drugs relieve symptomatic pain only without affecting its cause. The methyl sulfones **2** and **7**, which presented an interesting anti-inflammatory activity, were selected for the evaluation of analgesia. The analgesic effect of methyl sulfones **2** and **7** was investigated using acetic acid induced writhing method (chemical model of nociception). In the present study, analgesic activity was detected by measuring a decrease in the frequency of writhing and the

analgesic activity was correlated with the ability of the compounds to neutralize the pain sensation. The percentage inhibition of writhing by an analgesic compound is calculated according to the following formula:

Average withers in control group - Average withers in treated group ×100

100% Inhibition = Average withers in control group

Table 3. *In vivo* Analgesic Activity

Entry	Compound	Dose (mg/Kg)	Abdominal writhing	% Inhibition
1	Saline solution	0.0	21.70±1.12 n = 7	0.00
2	**2**	10	11.00±1.91 n = 4	49.34±8.81
3	**2**	20	9.50±1.31 n = 6	56.25±6.03
4	**2**	70	8.66±1.52 n = 6	60.09±7.00
5	**7**	10	11.75±1.65 n = 4	45.89±7.60
6	**7**	20	10.75±0.85 n = 4	50.49±3.93
7	**7**	70	7.62±1.17 n = 16	64.88±5.43
8	*Ibuprofen*	10	11.28 n = 4	48.01±5.25
9	*Ibuprofen*	20	10.20±1.87 n = 6	52,98±5.82

10	*Ibuprofen*	70	7.23±1.21	66.72±3.44
			n = 6	

n = number of mice used for every experiment. A dose of 10, 20 and 70 mg/Kg of every compound was administered. The abdominal writhing and % inhibition are expressed as mean values ± S.E.M. of at least four mice. Each test is indicative of statistically significant differences (P<0.05; one way ANOVA followed by Student-Newman-Keuls test)

Our results revealed significantly reduction of writhing with regards to the control study for **2** and **7**, reduction of the frequency of writhing approximately 45 and 64%, respectively (Table 3). The experimental data evidence obtained in the present study indicates that the methyl sulfones **2** and **7** possess time dependent analgesic activity in the tested experimental animals, with both compounds able to reduce contractions by 60 % at a dose of 70 mg/Kg.

In vivo gastrointestinal side effects

Gastrointestinal damage by NSAIDs is a commonly observed problem especially for those people with chronic diseases that must take NSAIDs over longer periods of time. Here, the study was carried out to determine the effect of methyl sulfones on the gastrointestinal section in rats. Gastric ulcers were not observed for any of two evaluated compounds and the treated animals did not suffer from any toxic side effects apart from minor hyperemia associated with treatment of compound **2** (Table 4, entry 1).

Table 4. *In vivo* gastrointestinal Activity

Entry	Compound	Rat weight (g)	Volume administrated (mL)	Gastric ulcers
1	**2**	170.0	1.70	*
2	**2**	170.5	1.70	0
3	**2**	155.9	1.56	0

4	**7**	180.4	1.80	0
5	**7**	181.2	1.81	0
6	**7**	175.2	1.75	0
7	**carboxymethylcellulose**	200.6	2.00	0
8	**carboxymethylcellulose**	185.1	1.85	0
9	**Saline solution**	180.3	1.80	0
10	**Saline Solution**	189.0	1.89	0

* Light hyperemia. A lot of 3 rates for every experiment has been used. A 70 mg/Kg of compound to tester was administered in suspension on carboxymethylcellulose at 0.5%.

A desirable anti-inflammatory treatment would maintain efficacy and minimize the gastric side effects. One of the aims of this work was to limit the undesired gastric effects of classical NSAIDs, theoretically related to the COX-1 inhibition. The decrease in GI effects can be attributed to the difference in acidity, so while ibuprofen has a pK_a ~ 4.8, the aryl methyl sulfones have pK_a ~ 28-30 in aqueous solution.[22]

Chemosensitivity

To evaluate if the most promising compounds **2**, **5** and **7** possessed inherent cytotoxic properties they were assessed in the human HT29 colon adenocarcinoma cell line using the MTT assay (Table 5). No IC_{50} values were obtained below 200 μM indicating no antiproliferative activity under the conditions investigated. Taken together with the data obtained from the in vivo gastrointestinal investigation it suggest a promising starting point for further optimization of novel sulfones possessing good anti-inflammatory activity and lacking off-target toxicity.

Table 5. Growth inhibition of aryl methyl sulfones analogues against HT29 cancer cells

Entry	**Compound**	**HT29 [μM]**

1	**2**	>200[a]
2	**5**	>200
3	**7**	>200
4	***oxaliplatin***	0.92 ± 0.25

[a]IC_{50} values for all compounds are the mean ± SD of at least three independent assays

2.3. Molecular Modeling

The carboxylic acids bind more strongly than methyl sulfone analogues while keeping the same binding mode

Molecular modeling can provide valuable information about the ligand-receptor binding mode and its associated relative free energies of binding of a series of inhibitor compounds. As validation for the simulation protocol adopted by the present work, we initially reproduced the crystallographic binding mode of ibuprofen in the COX-2 receptor (PDB code 4PH9). The superposition of the crystallographic binding mode of ibuprofen in COX-2 and the final structure of the corresponding modeled protein-ligand complex of compound **3** in the molecular dynamics showed satisfactory results (Figure 5).

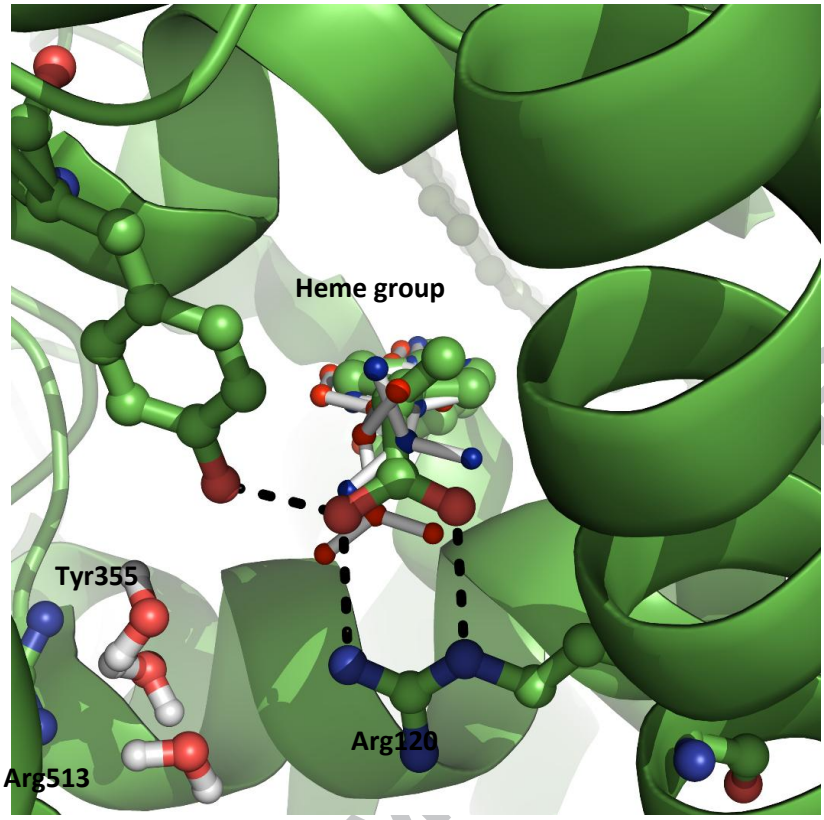

Figure 5. Superposition of experimental and simulated ibuprofen and its sulfone analogue in the binding site of mouse COX-2. Secondary structure elements and the bold ball & sticks representation correspond to crystal structure of ibuprofen bound to COX-2 (pdb code 4PH9). Thin balls & sticks representation correspond to ibuprofen (red spheres) and its methyl sulfone analogue (compound **3**, blue spheres)

Likewise, the replacement of the carboxylate group by the methyl sulfone moiety in the ibuprofen skeleton also yielded a stable complex structure (Figure 5), whose structural integrity is maintained through the polar interaction between the sulfone group and both Arg120 and Tyr355 residues. Therefore, like ibuprofen, its sulfone analogue also blocks the entrance of the substrate to the catalytic site of COX-2 as Figure 5 shows. However the fluctuation of the sulfone analogue ligand at the interior of the binding cavity is significantly higher than that of the carboxylate analogue (see Figure S1). From the energetic point of view, the comparison of the binding free energies of these two inhibitors also confirmed the significantly lower affinity of the sulfone analogue **3** compared with its carboxylic analogue by a difference of 9.6 kcal/mol according to MM-PBSA, 5.0 kcal/mol according to MM-GBSA and 15.4 computed with MM-

3DRISM (entry 7 and 8 in Table 6 and Table S1). Experimentally, the same trend was observed with a 15-fold decrease in affinity for ibuprofen (IC_{50} = 1.5 μM, entry 7 in Table 2) when compared with its sulfone analogue **3** (IC_{50} = 22.05 μM, entry 5 in Table 2). In other words, if the binding mode is maintained when comparing carboxylate and sulfone analogues, a decrease of affinity is expected since the sulfone group acts as a weaker binder (less polar) to Arg120 at the entrance of the binding site compared to the carboxylate group. Similarly the replacement of the carboxylic acid group by the methyl sulfone in a bulky 1,5-biaryl pyrrole EP1 receptor antagonist significantly reduced the binding affinity, in line with the present results.[23]

Table 6. Experimental and calculated binding free energies (kcal/mol) at different binding modes for all studied sulfone derivatives and reference inhibitors ibuprofen and celecoxib

Entry	Compound	$\Delta G_{bind,exp}$ [a]	Binding mode [b]	MD simulations [c]	$\Delta G_{bind,MM-PBSA}$
1	**2**	-9.5	1	2 x 120 ns	-14.7 ± 2.7
			2	2 x 60 ns	-13.6 ± 2.2
			3	2 x 60 ns	-11.8 ± 2.8
2	**1**	-8.9	1	1 x 120 ns	-15.8 ± 2.5
			2	1 x 60 ns	-15.6 ± 2.4
			3	1 x 60 ns	-12.3 ± 2.8
3	**7**	-8.4	1	1 x 60 ns	-12.9 ± 2.8
			2	1 x 60 ns	-14.9 ± 2.8
			3	1 x 60 ns	-11.0 ± 2.7
4	**5**	-8.3	1	1 x 60 ns	-22.5 ± 3.0
5	**4**	-7.8	1	1 x 60 ns	-17.6 ± 2.9
6			2	1 x 60 ns	-15.7 ± 2.3

7	**6**	-6.7	1	1 x 60 ns	-15.7 ± 3.0
8	**3**	-6.3	1	1 x 60 ns	-13.5 ± 2.4
9	Ibuprofen	-	1	1 x 60 ns	-23.1 ± 3.1
10	Celecoxib	-	2	1 x 60 ns	-24.9 ± 3.0

[a]Computed using $\Delta G_{bind,exp} = -R \cdot T \cdot \ln(1/IC_{50})$, [b)]Mode 1 = ibuprofen-like binding mode, PDB code 4PH9, Mode 2 = celecoxib-like binding mode, PDB code 3LN1 and mode 3 = diclofenac-like binding modem PDB code 1PXX. [c]Number of simulations x extension of the simulation.

Molecular modeling of the COX-2 inhibitory action of Methyl Sulfones analogues

The comparison of the experimental versus simulated binding free energies for all sulfone analogues is displayed in Figure 6 for MM-PBSA (Table S1, Figure S2 and S3 for the corresponding MM-GBSA and MM-3DRISM results, respectively). Two different groups are differentiated and confirmed in all three methodologies. The binding free energies of less active inhibitors, compounds **3**, **5** and **6** (analogues of ibuprofen, indomethacin and ketoprofen, respectively), based on the ibuprofen-like binding mode correlated with experimental binding affinity whereas, on the contrary, no correlation was found for the most active inhibitors, compounds **1**, **2**, **4** and **7** (analogues of fenoprofen, naproxen, metiazinic acid and ketoprofen). Compounds **3**, **5** and **6** (hereafter named as correlated compounds) would adopt the ibuprofen-like binding mode (mode 1) like the corresponding parent compounds ibuprofen (PDB code 4PH9) and indomethacin (PDB code 4COX. This mode is characterized by hydrogen bonding interactions of the oxygen atoms of the sulfone group with Arg120 and Tyr355 and also transitory hydrogen bond contacts between hydroxyl group of Ser530 and the ketone group of compounds 5 and 6. Furthermore, the ibuprofen-like binding mode involves favorable hydrophobic contacts with Ala527, Val523, Val349, Leu352, Ser353, Ala527 and Leu531 at the entrance of the binding channel for all these inhibitors and with Phe518 at the rear part of the binding site as shown by the per-residue decomposition of the binding free energy in Table S2

and the representation of the ibuprofen-like binding mode in Figure 7. The higher affinity of compound **5** over **3** and **6** can be attributed to the most favorable hydrophobic interaction energy (see ΔE_{vdw} term in Table S3) at the entrance of the cavity for the most bulky compound **5** compared to the smaller ones (**3** and **6**). It is also important to note that the role of the bridged water molecule between Ser530 and Tyr385 (see Figure **7**) at the rear part of the cavity provides remarkable structural stability to the binding site. This highly stable water molecule with long lifetimes is also present in the crystal structure of ibuprofen bound to COX-2 (PDB code 4PH9).[24]

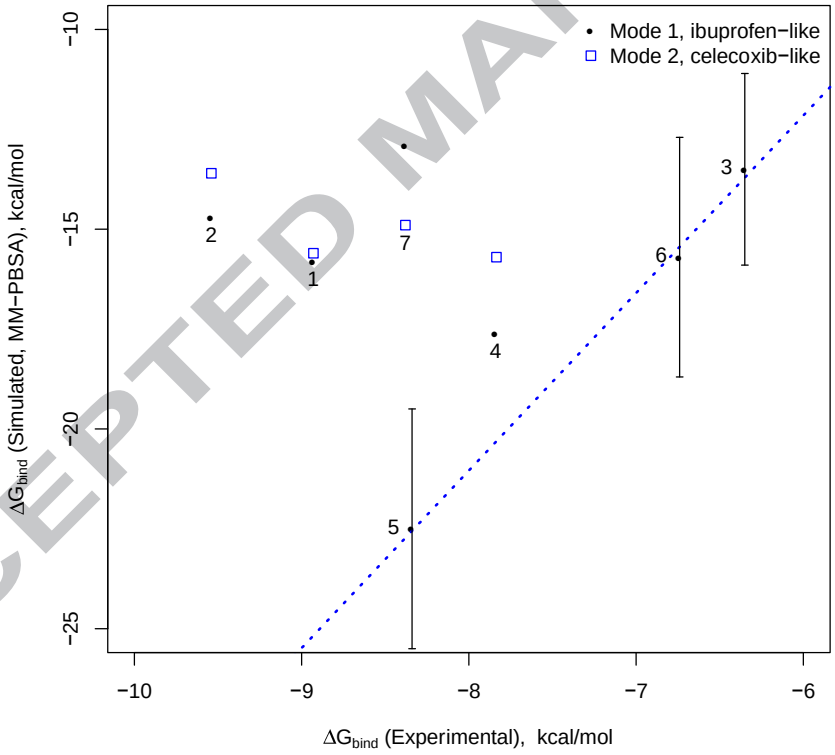

Figure 6. Correlation between COX-2 experimental and simulated MM-PBSA binding free energies (ΔG_{bind}) for all methyl sulfone derivative inhibitors. Black circles correspond to the binding free energies simulated at binding mode 1 (ibuprofen-like) whereas the empty blue squares represent binding mode 2 (celecoxib-like). Compounds **3**, **5** and **6** correlate to the experimental values and compounds **1**, **2**, **4** and **7** identify the uncorrelated compounds.

The uncorrelated binding free energies computed at the binding mode 1 (ibuprofen-like) for the most active inhibitors prompted us to explore other binding modes for these compounds (**1**, **2**, **4**

and **7**, hereafter named as uncorrelated compounds), like that found for celecoxib (pdb code 3LN1, mode 2) and diclofenac (pdb code 1PXX, mode 3).

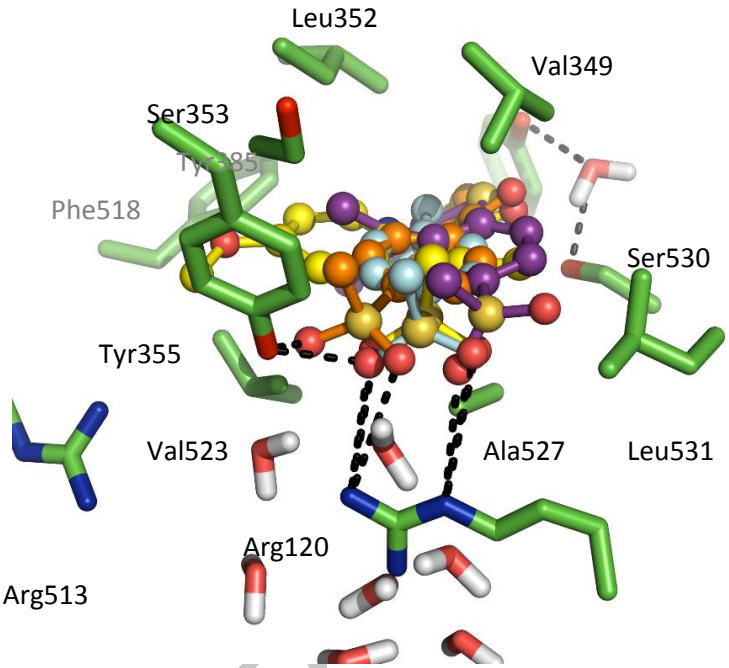

Figure 7. Superposition of sulfone analogue structures that its calculated binding free energies correlate to the experimental values in the binding mode 1 (ibuprofen-like), compounds **3**, **5** and **6**. Ligands are shown in balls & sticks with stick and carbon atom colors indicating each compound (**3**/marine blue, **5**/yellow and 6/orange). Compound **4** (purple) is also added to the representation. The 10 most important residues in the stabilization of such binding mode are shown in green sticks see also Table S2. Additionally Ser530, Tyr385 and Arg513 are also shown. Most important hydrogen bonds are also indicated with a dotted line.

Celecoxib-like binding mode is characterized by the polar interaction between the sulfone group and Arg513 instead of Arg120 and also hydrophobic contacts with Phe518, Ile517 and Ala516 in addition to the same hydrophobic residues listed for ibuprofen-like binding mode at the entrance of the binding channel except Leu531 which is located far away from the cavity (see Figure 8 and Table S4). Likewise, transitory hydrogen bonds between the ketone group of compound **2** and Ser530 are observed. Meanwhile, the diclofenac-like binding mode orients the sulfone group towards Ser530 at the rear part of the binding site. Even though any of the new explored binding modes provided a significant enhancement of the binding affinity, celecoxib-like binding mode emerges as a competitive binding mode to ibuprofen-like binding mode for the four uncorrelated

compounds. The computed energy difference between both binding modes ranges only from -0.2 to -2.0 kcal/mol computed at MM-PBSA level for these inhibitors, which corroborate its similar stability. It is remarkable that three out of four of these compounds (**1**, **2** and **4**) are precisely those that the substitution of the carboxylate for a sulfone group causes an increment of their activity, unlike to the correlated compounds (**3** and **6**), see Figure 4. On the other hand, notice that compounds **5** and **7** do not alter their activities compared to the carboxylate analogue compounds. In the case of the bulky indomethacin (compound **5**) the conservation of the activity after the substitution of the acidic group by a methyl sulfone would indicate the prominence of the hydrophobic skeleton in the magnitude of the binding affinity. Taken into account that this substitution, while keeping the same binding mode, yields a reduction in affinity (as seen in the ibuprofen example above), it is a clear indication that, indeed, these uncorrelated sulfone compounds change their binding mode or binding mechanism in full agreement with the simulated data presented here. However, unfortunately the new explored binding modes are not able to reproduce the final ranking, which could be indicative of the drawbacks of the present computational methodologies to estimate accurate binding free energies[25] or more probably that other mechanisms are in place for these tight-binding sulfone compounds. One well-known but poorly explained alternative mechanism for tight binding inhibitors that could explain the behavior of the top binders consists of a time-dependence mechanism of binding. This mechanism has been described for celecoxib in COX-2[26] and for flurbiprofen in COX-1, which seems to involve the stabilization of a competing conformational substrate of the enzyme.[27]

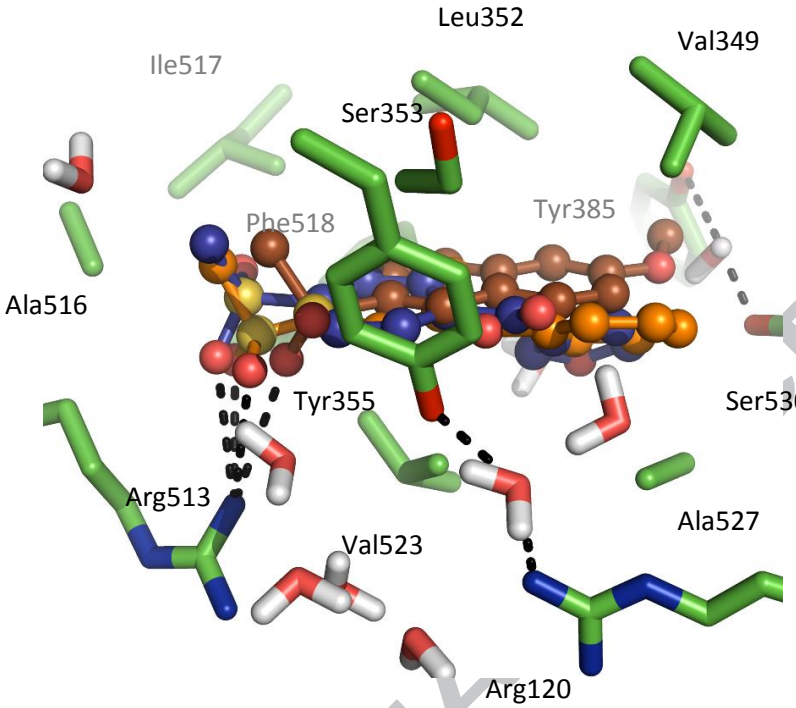

Figure 8. Superposition of sulfone analogue structures in the binding mode 2 (celecoxib-like) for compounds **1**, **2** and **7**. Ligands are shown in balls & sticks with stick and carbon atom color indicating each compound (**1**/orange, **2**/brown and **7**/deep blue). The most important residues in the stabilization of such binding mode are shown in green sticks. Additionally Ser530, Tyr385 and Arg120 are also shown. Most important hydrogen bonds are also indicated with a dotted line.

To sum up, the ibuprofen-like binding mode is expected for inhibitors that are less active than the carboxylate analogues whereas a different mechanism or binding mode is predicted for more active inhibitors than the carboxylate analogues. So, on the one hand, for the less active sulfone compounds the ibuprofen-like binding mode is maintained, and as a consequence of it, the hydrophobic interactions at the entrance of the binding channel dominate and determine the ranking of affinities of the methyl sulfone analogues. On the other hand, the unexpected high affinity of the most active sulfone analogues might be induced by a time dependent character of the protein-ligand binding.

3. Conclusion

We have synthesized and evaluated a series of methyl sulfones possessing anti-inflammatory properties. Results showed that the tested compounds (**1**-**7**) exhibited promising anti-

inflammatory activity compared to the parent drugs, with marked decreases in the ulcerogenic side effects. The peripheral analgesic effect of these methyl sulfones may also be mediated via inhibition of cyclooxygenase isoforms. Compounds **2** and **7** exert significant anti-inflammatory and anti-nociceptive effects in tested mice while they are not toxic at high doses. These results justify the study of methyl sulfones as a new class of NSAIDs that exhibit an interesting anti-inflammatory activity profile. Finally, the results of the *in vivo* anti-inflammatory activity by the standard acute carrageenan-induced paw edema method in rats, revealed remarkable activity for compounds **1**, **2, 5** and **7**. Molecular modeling studies found a significant decrease of the COX-2 binding affinities of the sulfone derivatives compared to their carboxylate analogues while keeping the same binding mode, as a consequence of that, the most active compounds **(1**, **2**, **4** and **7)** would accomplish their inhibitory activities through a different binding site or mechanism than the less active compounds **(3**, **5** and **6)** whose binding site would correspond to that found for ibuprofen (4PH9, polar moiety of the inhibitor compound oriented to the mouth of the binding cavity). Such increment of the inhibitory activity would be performed through a change of the binding mode or mechanism compared to the standard ibuprofen binding site. Unfortunately, the inhibitor structure does not provide any evidence of rationalization of such behavior.

Compound **2** the most relevant methyl sulfone of these series exhibited superior inhibition of COX-1 (IC_{50} = 0.04 μM) and COX-2 (IC_{50} = 0.10 μM) compared with that of naproxen (COX-1 (IC_{50} = 11.30 μM) and COX-2 (IC_{50} = 3.36 μM) *in vitro* and better reduction of inflammation than ibuprofen *in vivo*. It also demonstrated a good oral absorption and long duration of anti-inflammatory effect (34.6% of inhibition after 4 h of administration of a 70 mg/Kg dose in rat). No detectable toxicity against HT29 human cells, interesting analgesic activity and non ulcerogenic effect under the tested conditions were other properties of compound **2**, which showed a promising pharmacological profile. The results reveal that the replacement of

carboxylic acid by methyl sulfone in classical NSAIDs may be a promising approach to design new COX inhibitors with anti-inflammatory and analgesic properties and reduced gastrointestinal side effects.

4. Experimental Section

4.1. Chemistry

Microwave assisted reactions were carried using a CEM Discover LabMate instrument and the temperature vessel was measured by an IR sensor. The reactions were monitored by thin-layer chromatography (TLC) analysis using silica gel (60 F254, Merck) plates. Compounds were visualized by UV irradiation. Column chromatography was performed with silica gel 60 (230-400 mesh, 0.040-0.063 mm) and automatic column chromatography was performed with a CombiFlash R_f system with UV-*vis* (PN 68-5230-008) detector and RediSep R_f 4 and 12 g silica gel column. Melting points (mp) were obtained on a MFB-595010M Gallenkamp apparatus with digital thermometer in open capillary tubes and are reported without correction. IR spectra were obtained using FTIR Perkin-Elmer 1600 Infrared Spectrophotometer. ^{1}H and ^{13}C NMR spectra were recorded on a Varian Gemini-400 (100 MHz). Chemical shifts are reported in parts per million (ppm) relative to the central peak of the solvent: $CDCl_3$ (δ, 7.26 (H) and 77.00 (C)), CD_3OD (δ, 3.31 (H) and 49.45 (C)), DMSO-d_6 (δ, 2.49 (H) and 39.51 (C)) as internal standards. The following abbreviations are used for the proton spectra multiplicities: s, singlet, d, doublet, t, triplet, q, quadruplet, m, multiplet. Coupling constants (*J*) are reported in Hertz (Hz).

The purities of all isolated compounds were determined by electrospray ionization (ESI-HMRS)-mass spectra on a LC/MSD-TOF (2006) (Agilent technologies) by the «Section of spectrometry of masses » at the University of Barcelona. The purity of the compounds proved to be >95%. All reagents were of high quality or were purified before use. Organic solvents were of analytical grade or were purified by standard procedures.

*4.2. 3-Phenoxy-1-methylsulfonylbenzene (**1**).* Aryl halide **9** (0.080 g, 0.34 mmol), phenol (0.048 g, 0.5 mmol), Cs_2CO_3 (0.300 g, 0.6 mmol), ACNH and CuBr in catalyst amount (0.1%) in DMF (10 mL) were added to the microwave tube. The mixture was reacted in a microwave oven (CEM Discover LabMate) at 100 ºC (external temperature) for 1 hour and was monitored by TLC. After completion of the reaction, it was cooled to room temperature; H_2O (10 mL) was added and then the crude of reaction was extracted with ethyl ether (3 x 15 mL). The combined organic extracts were washed with water (3 x 15 mL) and dried over Na_2SO_4. After removal of the solvent, the residue was purified by automatic column chromatography CombiFlash R_f with UV-*vis* detector using 12 g silica gel column and eluting with a stepwise gradient (Hexane:EtOAc, 1:0 → 0:1) to give a yellow oil. 98% (83 mg) yield; IR (ATR diamond, cm-1) υ: 1447, 1301, 1231, 1142, 753, 683; ^{1}H NMR (400 MHz, $CDCl_3$) δ: 3.04 (s, 3H, CH_3), 7.04 (d, *J* = 8.4Hz, 2H, H-2', H-6'), 7.20 (t, *J* = 7.6Hz, 1H, H-4'), 7.25 (d, *J* = 8Hz, 1H, H-4), 7.40 (t, *J* = 8.4Hz, 2H, H-3', H-5'), 7.52 (t, *J* = 8.4Hz, 1H, H-5), 7.53 (s, 1H, H-2), 7.64 (d, *J* = 8Hz, 1H, H-6); ^{13}C NMR (100 MHz, $CDCl_3$) δ: 44.7 (CH_3), 116.9 (CH), 120.0 (2CH), 121.7 (CH), 123.6 (CH), 125.5 (CH), 130.5 (2CH), 131.2 (CH), 142.4 (Cq), 155.9 (Cq), 158.8 (Cq); HRMS (ESI): calcd for $C_{13}H_{13}O_3S$ $[M+H]^+$: 249.0585 found 249.0592.

4.3. General procedure of oxidation with m-CPBA

To a solution of the sulfone (1 mmol) in dichloromethane (20-25 mL) was added *m*-CPBA (2.5 mmol) at 0 ºC under argon atmosphere. The crude mixture was stirred at rt for 2 h before it was basified with 2N NaOH and extracted with dichloromethane (3x20 mL). Organic layers were dried (Na_2SO_4), filtered and concentrated under vacuum.

*4.4. Methylsulfonyl-6-methoxynaphthalene (**2**).* Following general procedure of oxidation with *m*-CPBA, the sulfone **2** was obtained from **11** as a yellow solid with 87% (227 mg) yield; mp: 132-134 ºC (dichloromethane); IR (ATR diamond, cm-1) υ: 1594, 1259, 1216, 1145; ^{1}H NMR (400 MHz, $CDCl_3$) δ: 3.11 (s, 3H, SCH_3), 3.97 (s, 3H, OCH_3), 7.20 (s, 1H, H-5), 7.28 (d, *J* = 9 Hz, 1H, H-7), 7.87–7.90 (m, 3H, H-3, H-4, H-8), 8.43 (s, 1H, H-1); ^{13}C NMR (100 MHz, $CDCl_3$) δ: 45.0(CH_3), 55.9 (CH_3), 106.2 (CH), 121.1 (CH), 123.2 (CH), 127.8 (Cq), 128.5 (CH), 129.1 (CH), 131.2 (CH), 135.3 (Cq), 137.4 (Cq), 160.5 (Cq); HRMS (ESI): calcd for $C_{12}H_{13}O_3S$ $[M+H]^+$: 237.0585 found 237.0573.

*4.5. 4-Isobutylphenyl methyl sulfone (**3**).* A mixture of zinc (3.76 g, 57.51 mmol), mercury (II) chloride (0.38 g, 1.44 mmol) and HCl concd (1 mL) in H_2O (3 mL) was stirred at room temperature for 5 min. Then, the crude mixture was filtered and the solid residue was treated with H_2O (0.5 mL), HCl concd (1.3 mL), toluene (1 mL) and the ketone **15** (2.9 g, 12.82 mmol). The reaction mixture was heated under reflux of water during 5 h. Then, the mixture was diluted with water (20 mL) and extracted with diethyl ether (3× 20 mL). The combined organic layers were washed with H_2O (20 mL) and dried with Na_2SO_4. The drying agent was filtered off and the filtrate was evaporated to dryness to afford a brown oil. The crude reaction was purified by automatic column chromatography CombiFlash R_f with UV-*vis* detector using 12 g silica gel column and eluting with stepwise gradient (Hexane:EtOAc, 1:0 → 0:1) to give a yellow oil. 22% (260 mg) yield; IR (ATR diamond, cm-1) υ: 1596, 1257; ^{1}H NMR (400 MHz, $CDCl_3$) δ: 1.08 (d, *J* = 6 Hz, 6H, CH_3 (x2)), 2.02 (sept, *J* = 6 Hz, 1H, CH-($(CH_3)_2$), 2.61 (d, *J* = 6 Hz, 2H, CH_2-Ar), 2.65 (s, 3H, SO_2CH3), 7.24 (d, *J* = 9 Hz, 2H, H-3,H-5), 7.38 (d, *J* = 9 Hz, 2H, H-2,H-6); ^{13}C NMR (100 MHz, $CDCl_3$) δ: 16.7 ($2CH_3$), 22.7 (CH_3), 30.1 (CH), 45.2 (CH_2), 127.3 (2CH), 130.0 (2CH), 135.3 (Cq), 139.2 (Cq); HRMS (ESI): calcd for $C_{11}H_{17}O_2S$ $[M+H]^+$: 213.0949 found 213.0954.

*4.6. 10-Methyl-2-methylsulfonyl-10H-phenothiazine (**4**).* To a stirred solution of methyl sulfone **18** (0.096 g, 0.35 mmol) in 7 mL of DMF cooled at 0 °C was added a solution of NaH 60% (0.014 g, 0.35 mmol) in 3 mL of DMF. Next, iodomethane (0.024 mL, 0.39 mmol) was added to the crude mixture and stirred at room temperature for 24 h before the crude reaction was diluted with ice-cold H_2O and extracted with diethyl ether and H_2O (2:1). The organic layers were dried with Na_2SO_4, filtered off and concentrated under reduced pressure. The crude reaction was purified by automatic column chromatography CombiFlash R_f with UV-*vis* detector using 12 g silica gel column and eluting with stepwise gradient (Hexane:EtOAc, 1:0 → 0.8:0.2) to give a green solid with 71% (72 mg) yield; mp: 130-132 ºC (hexane/ethyl acetate); IR (ATR diamond, cm-1) υ: 1562, 1292; ^{1}H NMR (400 MHz, $CDCl_3$) δ: 2.99 (s, 3H, NCH_3), 3.38 (s, 3H, SO_2CH_3), 6.83 (d, *J* = 6 Hz, 2H, H-4, H-6), 6.97 (t, *J* =6 Hz, 1H, H-7), 7.09 (d, *J* = 6 Hz, 1H, H-9), 7.18 (t, *J* = 6 Hz, 1H, H-8), 7.60 (s, 1H, H-1), 7.67 (d, *J* = 6 Hz, 1H, H-3); ^{13}C NMR (100 MHz, $CDCl_3$) δ: 35.8 (CH_3), 44.8 (CH_3), 113.7 (CH), 114.9 (CH), 122.1 (CH), 123.7 (Cq), 124.7 (CH), 125.9 (Cq), 127.28 (CH), 127.30 (CH), 128.0 (CH), 133.6 (Cq), 144.1 (Cq), 150.4 (Cq); HRMS (ESI): calcd for $C_{14}H_{14}NO_2S_2$ $[M+H]^+$: 292.0466 found 292.0458.

*4.7. 2-Methyl-3-sulfonyl-5-methoxy-1-(p-chlorobenzoyl)indole (**5**).* To a stirred solution of methyl sulfone **22** (0.099 g, 0.41 mmol) in 7 mL of ice-cold DMF was added a solution of NaH 60% (0.024 g, 0.60 mmol) in 3 mL of DMF. After 30 min of stirring at 0 °C, 4-chlorobenzoyl chloride (0.053 mL, 0.41 mmol) was added and the reaction was allowed to warm up to room temperature and stirred for 24 h. Next, the solution was diluted with H_2O (20 mL) and extracted with diethyl ether (3x20 mL). The combined organic layers were washed with H_2O (20 mL) and dried with Na_2SO_4. The drying agent was filtered off and the filtrate was evaporated to dryness. The crude reaction was purified by automatic column chromatography CombiFlash R_f with UV-

vis detector using 12 g silica gel column and eluting with stepwise gradient (Hexane:EtOAc, 1:0 0.8:0.2 to give a dark yellow solid in 29% (46 mg) yield; mp: 133-135 °C (hexane/ethyl acetate); IR (ATR diamond, cm-1) υ: 1677, 1584, 1280), 1208, 1115, 755; ^{1}H NMR (400 MHz, DMSO-d_6) δ: 2.76 (s, 3H, CH_3-Ar), 3.42 (s, 3H, SO_2CH_3), 3.95 (s, 3H, OCH_3), 6.99 (d, *J* = 6 Hz, 1H, H-6), 7.09 (d, *J* = 6 Hz, 1H, H-7), 7.53 (s, 1H, H-4), 7.82 (d, *J* = 9 Hz, 2H, C-3', C-5'), 7.93 (d, *J* = 9 Hz, 2H, C-2', C-6'); ^{13}C NMR (100 MHz, DMSO-d_6) δ: 13.7 (CH_3), 45.4 (CH_3), 55.9 (CH_3), 102.3 (CH), 113.6 (CH), 115.2 (CH), 117.2 (Cq), 118.0 (Cq), 126.2 (Cq), 127.0 (Cq), 149.8 (Cq), 143.8 (CH), 156.5 (CH), 168.4 (Cq); HRMS (ESI): calcd for $C_{18}H_{17}ClNO_4S$ $[M+H]^+$: 378.0567 found 378.0561.

*4.8. (4'-Chlorophenyl)(4-methylsulfonyl)phenyl)methanone (**6**).* Following general procedure of oxidation with *m*-CPBA, the sulfone **6** was obtained from **24** as a brown solid with 99% (1.68 g) yield; mp: 163-171 ºC (hexane/ethyl acetate); IR (ATR diamond, cm^{-1}) υ: 1651, 1583, 1284, 746; ^{1}H NMR (400 MHz, $CDCl_3$) δ: 3.12 (s, 3H, SCH_3), 7.50 (d, *J* = 6 Hz, 2H, H-3', H-5'), 7.76 (d, *J* = 6 Hz, 2H, H-2', H-6'), 7.93 (d, *J* = 6 Hz, 2H, H-3, H-5), 8.09 (d, *J* = 6 Hz, 2H, H-2, H-6); ^{13}C NMR (100 MHz, $CDCl_3$) δ: 44.7 (CH_3), 123.9 (Cq), 127.9 (2CH), 129.3 (2CH), 130.8 (2CH), 131.8 (2CH), 134.9 (Cq), 142.2 (Cq), 144.0 (Cq), 194.2 (Cq); HRMS (ESI): calcd for $C_{14}H_{12}ClO_3S$ $[M+H]^+$: 295.0196 found 295.0203.

*4.9. Furan-3-yl-(4-(methylsulfonyl)phenyl)methanone (**7**).* Following general procedure of oxidation with *m*-CPBA, the sulfone **7** was obtained from **26** as an orange solid with 95% (109 mg) yield; mp: 125-127 ºC (hexane/ethyl acetate); IR (ATR diamond, cm-1) υ: 1648, 1562, 1293, 1234, 1142; ^{1}H NMR (400 MHz, $CDCl_3$) δ: 3.13 (s, 3H, SCH_3), 6.92 (d, *J* = 1.4 Hz, 1H, H-4'), 7.56 (d, *J* =1.4 Hz, 1H, H-5'), 7.95 (s, 1H, H-2'), 8.01 (d, *J* = 9 Hz, 2H, H-3, H-5), 8.09 (d, *J* = 9 Hz, 2H, H-2, H-6); ^{13}C NMR (100 MHz, $CDCl_3$) δ: 44.7 (CH_3), 110.2 (CH), 126.5

(CH), 128.1 (2CH), 129.8 (2CH), 143.5 (Cq), 143.5 (Cq), 144.9 (Cq), 149.5 (Cq), 188.2 (Cq); HRMS (ESI): calcd for $C_{12}H_{11}O_4S$ $[M+H]^+$: 251.0378 found 251.0382.

*4.10. 6-Methylthio-2-methoxynaphthalene (**11**).* To a cooled solution (-78 °C) of the 2-bromonaphthalene **10** (0.40 g, 1.69 mmol) in anhydrous THF (5 mL) under an argon atmosphere, a 2 M solution of butyl lithium in hexane (1.3 mL, 2.6 mmol) was added dropwise with stirring over a 15-min period. The crude mixture was slowly stirred at -78 °C for 1 h, and dimethyl disulfide (0.2 mL, 2.22 mmol) was slowly added with stirring. The solution was allowed to warm to room temperature (20 °C) for 1 h and then hydrolyzed with saturated aqueous ammonium chloride solution (5 mL). The solution was extracted with diethyl ether (3x20 mL) and the extracts were dried with Na_2SO_4 and evaporated under reduced pressure. Product **11** was obtained as a yellow solid with 98% (312 mg) yield; ^{1}H NMR (400 MHz, $CDCl_3$) δ: 2.56 (s, 3H, SCH_3), 3.91 (s, 3H, OCH_3), 7.09 (s, 1H, H-1), 7.13 (d, *J* = 9 Hz, 1H, H-3), 7.37 (d, *J* = 9 Hz, 1H, H-4), 7.59 (s, 1H, H-5), 7.64 (d, *J* = 9 Hz, 2H, H-7, H-8); ^{13}C NMR (100 MHz, $CDCl_3$) δ: 16.8 (CH_3), 55.7 (CH_3), 106.2 (CH), 119.6 (CH), 124.8 (CH), 127.0 (CH), 127.5 (CH), 128.7 (CH), 129.8 (Cq), 132.9 (Cq), 133.4 (Cq), 157.7 (Cq). HRMS (ESI): calcd for $C_{12}H_{13}OS$ $[M+H]^+$: 205.0687 found 205.0685.

*4.11. 2-Methyl-1-(4-methylthiophenyl)propan-1-one (**14**).* Aluminium trichloride (2.5 g, 18.73 mmol) was added to a solution of isobutyryl chloride (2.02 g, 18.96 mmol) in dichloromethane (40 mL) and stirred at 0 °C for 10-15 min. Thioanisole **12** (2.00 g, 16.10 mmol) was added and the resulting mixture was stirred at room temperature for 24 h. The reaction mixture was acidified with 5N HCl and extracted with dichloromethane (3x20 mL). The organic layers were dried with Na_2SO_4, filtered off and concentrated under reduced pressure. The product was obtained as yellow oil. 93% (2.90 mg) yield; ^{1}H NMR (400 MHz, $CDCl_3$) δ: 1.20 (d, *J* = 6.9 Hz,

6H), 2.51 (s, 3H, SCH_3), 3.51 (sept, *J* = 6.9 Hz, 1H, CH), 7.27 (d, *J* = 9 Hz, 2H, H-3, H-5), 7.87 (d, *J* = 9 Hz, 2H, H-2, H-6); ^{13}C NMR (100 MHz, $CDCl_3$) δ: 14.9 (CH_3), 19.4 ($2CH_3$), 35.3 (CH), 125.2 (2CH), 128.9 (2CH), 132.6 (Cq), 145.0 (Cq), 203.5 (Cq). HRMS (ESI): calcd for $C_{11}H_{15}OS$ $[M+H]^+$: 195.0844 found 195.0848.

*4.12. 1-(4-Methylsulfonyl)-2-methylpropan-1-one (**15**).* Following general procedure of oxidation with *m*-CPBA, the sulfone **15** was obtained from **14** as a yellow oil in 78% (2.62 g) yield; ^1H NMR (400 MHz, $CDCl_3$) δ: 1.24 (d, *J* = 6.9 Hz, 6H, CH_3 (x2)), 3.10 (s, 3H, SCH_3), 3.56 (sept, *J* = 6.6 Hz, 1H, $CH(CH_3)_2$), 8.06 (d, *J* = 8.7 Hz, 2H, H-2, H-6), 8.12 (d, *J* =8.7 Hz, 2H, H-3, H-5); ^{13}C NMR (100 MHz, $CDCl_3$) δ: 19.8 ($2CH_3$), 36.2 (CH), 44.3 (CH_3), 128.3 (2CH), 129.4 (2CH), 131.2 (Cq), 141.5 (Cq), 169.0 (Cq). HRMS (ESI): calcd for $C_{11}H_{15}O_3S$ $[M+H]^+$: 227.0742 found 227.0745.

*4.13. N-Acetylphenothiazine (**17**).* A mixture of zinc chloride (0.75 g, 5.50 mmol), acetyl chloride (0.8 mL, 5.62 mmol) in dichloromethane (25 mL) at 0 °C was stirred for 20 min. Phenothiazine **16** (1.00 g, 5.02 mmol) was added to the solution and stirred at rt for 24 h before reaction mixture was diluted with ice-cold H_2O and extracted with dichloromethane (3x20 mL). The organic layers were dried with Na_2SO_4, filtered off and concentrated under reduced pressure. The product **17** was obtained as a green solid in 96% (1.146 g) yield; mp: 191-195 °C (dichloromethane); IR (ATR diamond, cm-1) υ: 1668, 1459, 1315, 1257; ^1H NMR (400 MHz, $CDCl_3$) δ: 2.20 (s, 3H, CH_3), 7.22 (t, *J* = 6 Hz, 2H, H-7, H-3), 7.32 (t, *J* = 6 Hz, 2H, H-2, H-8), 7.43 (d, *J* = 6 Hz, 2H, H-4, H-6), 7.50 (d, *J* =6 Hz, 2H, H-1, H-9); ^{13}C NMR (100 MHz, $CDCl_3$) δ: 23.4 (CH_3), 127.1 (2CH), 127.3 (2CH), 127.5 (2CH), 128.3 (2CH), 133.4 (2Cq), 139.3 (2Cq), 169.6 (Cq). HRMS (ESI): calcd for $C_{14}H_{12}NOS$ $[M+H]^+$: 242.0640 found 242.0638.

*4.14. 4-Methylsulfonylphenothiazine (**18**).* A mixture of aluminium trichloride (0.17 g, 1.24 mmol) and methanesulfonyl chloride (0.17 mL, 2.34 mmol) in dichloromethane (20 mL) at 0 °C was stirred for 15 min before compound **17** (0.30 g, 1.24 mmol) was added. The reaction mixture was stirred at rt for 24 h before it was diluted with ice-cold H_2O and extracted with dichloromethane (3x20 mL). The organic layers were dried with Na_2SO_4, filtered off and concentrated under reduced pressure. The crude product was purified by silica gel column chromatography using Hexane:EtOAc (0.65:0.35) as eluent. The product **18** was obtained as a green solid in 28% (96 mg) yield; mp: 211-215 °C (hexane/ethyl acetate); IR (ATR diamond, cm-1) υ: 3351, 1567, 1310, 1297; ^{1}H NMR (400 MHz, acetona-d_6) δ: 3.22 (s, 3H, CH_3), 6.90 (d, *J* = 9 Hz, 1H, H-9), 6.98 (d, *J* = 9 Hz, 1H, H-6), 7.03 (t, *J* = 9 Hz, 1H, H-7), 7.13 (d, *J* = 6 Hz, 1H, H-3), 7.20 (t, *J* = 9 Hz, 1H, H-8), 7.58 (s, 1H, H-1), 7.66 (d, *J* = 6 Hz, 1H, H-4), 8.55 (bs, 1H, NH-); ^{13}C NMR (100 MHz, acetone-d_6) δ: 44.2 (CH_3), 114.5 (CH), 115.6 (CH), 116.9 (Cq), 118.7 (Cq), 123.8 (CH), 125.9 (CH), 126.8 (CH), 127.8 (CH), 128.4 (CH), 134.7 (Cq), 140.9 (Cq), 147.2 (Cq). HRMS (ESI): calcd for $C_{13}H_{12}NO_2S_2$ $[M+H]^+$: 278.0309 found 278.0310.

*4.15. 2-Methyl-5-methoxy-3-iodo-1H-indole (**20**).* To a solution of indole **19** (0.10 g, 0.62 mmol) in DMF (2 mL) was added 2N KOH (1 mL) and the crude mixture was stirred for 20 min. Next, I_2 (0.157 g, 0.62 mmol) in DMF (2 mL) was added to the mixture and the resulting solution was stirred for 1 h. The residue was extracted with diethyl ether and H_2O (2:1) and the organic layers were dried with Na_2SO_4, filtered off and concentrated under reduced pressure. A yellow solid was obtained quantitatively in 100% (187 mg) yield; ^{1}H NMR (400 MHz, $CDCl_3$+$(CD_3)_2CO$) δ: 2.45 (s, 3H, CH_3-Ar), 3.88 (s, 3H, OCH_3), 6.80 (bs, 2H, H-4, H-7), 7.12 (bs, 1H, H-6), 8.10 (bs, 1H, NH); ^{13}C NMR (100 MHz, $CDCl_3$) δ: 14.9 (CH_3), 56.3 (CH_3), 59.1 (CH), 102.6 (CH), 111.8 (CH), 112.7 (Cq), 131.1 (CH), 131.7 (CH), 137.3 (CH), 155.2 (Cq). HRMS (ESI): calcd for $C_{10}H_{11}INO$ $[M+H]^+$: 287.9885 found 287.9832.

*4.16. 2-Methyl-3-methylthio-5-methoxy-1H-indole (**21**).* A 2M solution of butyl lithium in hexane (0.65 mL, 0.65 mmol) under argon atmosphere was added to a solution of substituted indole **20** (124 mg, 0.43 mmol) in anhydrous THF (5 mL) stirred at -78 °C. The mixture was stirred for 45 min at -78 °C before dimethyl disulphide (0.08 mL, 0.88 mmol) was added at the same temperature. The resulting mixture was allowed to warm up slowly to room temperature and stirred for 1 h. The solution was hydrolyzed with saturated ammonium chloride solution (5 mL) and the obtained product was extracted with diethyl ether (3x20 mL). The organic layer was washed with H_2O (3x20 mL) and the organic layer was dried with Na_2SO_4, filtered off and evaporated to dryness. The crude reaction was purified by automatic column chromatography CombiFlash R_f with UV-*vis* detector using 12 g silica gel column and eluting with stepwise gradient (Hexane:EtOAc, 1:0 $\rightarrow$ 0:1) to give a brown solid in 98% (87 mg) yield; ^{1}H NMR (400 MHz, $CDCl_3$) δ: 2.28 (s, 3H, CH_3-Ar), 2.53 (s, 3H, SCH_3), 3.92 (s, 3H, OCH_3), 6.84 (d, *J* = 6 Hz, 1H, H-6), 7.18 (s, 1H, H-4), 7.19 (d, *J* = 6 Hz, 1H, H-7), 7.98 (bs, 1H, NH); ^{13}C NMR (100 MHz, $CDCl_3$) δ: 12.5 (CH_3), 20.1 (CH_3), 56.3 (CH_3), 101.0 (CH), 104.3 (CH), 111.7 (CH), 112.0 (Cq), 130.4 (CH), 131.1 (CH), 140.0 (CH), 155.0 (Cq). HRMS (ESI): calcd for $C_{11}H_{14}NOS$ $[M+H]^+$: 208.0796 found 208.0794.

*4.17. 2-Methyl-3-methylsulfonyl-5-methoxyindole (**22**).* Following general procedure of oxidation with *m*-CPBA, the product **22** was obtained as a yellow solid in 99% (99 mg) yield; ^{1}H NMR (400 MHz, $CDCl_3$) δ: 2.72 (s, 3H, CH_3-Ar), 3.11 (s, 3H, SO_2CH_3), 3.88 (s, 3H, OCH_3), 6.89 (d, *J* = 6 Hz, 1H, H-6), 7.23 (d, *J* = 6 Hz , 1H, H-7), 7.39 (s, 1H, H-4). HRMS (ESI): calcd for $C_{11}H_{14}NO_3S$ $[M+H]^+$: 240.0694 found 240.0694.

*4.18. 4'-Chloro-4-methylthiobenzophenone (**24**).* To a solution of 4-chlorobenzoyl chloride (1.02 mL, 8.07 mmol) in 20 mL of dichloromethane cooled at 0 °C was added aluminum chloride (1.28 g, 9.63 mmol) and the mixture was stirred for 15 min. Next, the thioanisole (0.95 mL, 8.17 mmol) was added and the resulting mixture was stirred at room temperature for 24 h. The solution was washed with H_2O (3x20 mL) and the organic layers were dried with Na_2SO_4, filtered off and the filtrate was concentrated under reduced pressure. The product **24** was obtained as a white solid. 87% (1.84 g) yield; mp: 120-123 ºC (hexane/ethyl acetate). IR (ATR diamond, cm-1) υ: 1636, 1585, 1283, 749; ^{1}H NMR (400 MHz, $CDCl_3$) δ: 2.54 (s, 3H, SCH_3), 7.25 (d, *J* = 9 Hz, 2H, H-2, H-6), 7.26 (d, *J* = 8 Hz, 2H, H-3', H-5'), 7.46 (d, *J* = 9 Hz, 2H, H-3, H-5), 7.74 (d, *J* = 8 Hz, 2H, H-2', H-6'); ^{13}C NMR (100 MHz, $CDCl_3$) δ: 15.9 (CH_3), 124.2 (2CH), 128.9 (2CH), 130.6 (2CH), 130.7 (2CH), 133.4 (Cq), 136.4 (Cq), 139.5 (Cq), 146.1 (Cq), 194.8 (Cq). HRMS (ESI): calcd for $C_{14}H_{12}ClOS$ $[M+H]^+$: 263.0297 found 263.0299.

*4.19. Furan-3-yl-(4-(methylthio)phenyl)methanone (**26**).* Titanium tetrachloride (0.15 mL, 1.36 mmol) was added to a solution of thioanisole **12** (127 mg, 1.02 mmol) in dichloromethane (15 mL) at 0 ºC under argon. Next, a solution of **25** (0.104 g, 0.80 mmol) in dichloromethane (2 mL) was added and the reaction mixture was stirred at room temperature for 10 h. The crude was diluted with ice-cold H_2O and the solution was washed with $NaHCO_3$. The organic layers were dried with Na_2SO_4, filtered off and concentrated under reduced pressure to give a solid which was purified by silica gel column chromatography using Hexane:EtOAc (0.8:0.2) as eluent. The product **26** was obtained as a white solid in 92% (235 mg) yield; mp: 132-136 °C (hexane/ethyl acetate); IR (KBr) υ (cm^{-1}): 1654, 1224, 1102; ^{1}H NMR (400 MHz, $CDCl_3$) δ: 2.42 (s, 3H, SCH_3), 6.97 (d, *J* = 1.5 Hz, 1H, H-4), 7.24 (m, 4H, Ar), 7.62 (s, 1H, H-2), 7.98 (d, *J* =1.5 Hz, 1H, H-5). HRMS (ESI): calcd for $C_{12}H_{11}O_2S$ $[M+H]^+$: 219.0480 found 219.0487.

5. Pharmacological methods

5.1. In vitro anti-inflammatory activity assay

The ability of the test compound to inhibit the conversion of arachidonic acid to prostaglandin H_2 (PGH_2) was determined using a COX-1/COX-2 inhibitor screening assay kit (cat. N. 560101; Cayman Chemical, Ann Arbor, MI)[19] The experimental procedure was approved by Animal Ethics Committee Generalitat de Catalunya (Spain). Briefly, COX catalyzes the first step in the biosynthesis of arachidonic acid to PGH_2. The COX (ovine) Inhibitor Screening Assay directly measures $PGF_{2\alpha}$ produced by $SnCl_2$ reduction when using an enzyme immunoassay (ACE competitive EIA). This assay is based on the competition between PGs and PG-acetylcholinesterase (AChE) conjugate (PG-tracer) for a limited amount of PG monoclonal antibody. Because the concentration of PGs varies, the amount of PG-tracer that is able to bind to the PGs monoclonal antibody will be inversely proportional to the concentration of PGs in the well. This antibody-PG complex binds to goat polyclonal anti-mouse IgG that has been previously attached to the well. The plate was washed to remove any unbound reagents and the Ellman's Reagent (which contains the substrate to acetylcholinesterase) is added to the well. The product of this enzymatic reaction absorbs at 405 nm. The intensity of this color, determined spectrophotometrically, is proportional to the amount of PG-trace bound to the well, which is inversely proportional to the amount of free PG present in the well during the incubation: Absorbance$\propto$ [bound PG-tracer]$\propto$1/[PGs].

5.2. In vivo assay

The carrageenin-induced rat paw oedema assay was carried out using a modified Winter's method as a preliminary screening test.[21] The rats (in groups of six animals weighing 160-200 g,

young adult male Sprague-Dawley) were starved for 24 h before the test compound (70 mg/Kg po) was administered. The drugs were dosed orally one hour before carrageenan evaluation. Rat paw edema was induced by subplantar injection of 0.1 mL of a 1% solution of carrageenan in sterile pyrogen-free 0.9% NaCl solution and the volume of paw was measured by water displacement in a plethysmometer (S-5128, Ugo Basile). Three and four hours after the injection of carrageenan, the volume of the paw was again measured. All statistical analyses of data were processed using software analysis (one way ANOVA followed by Student-Newman-Keuls test). Any treatments mean significantly less than the control mean was indicative of significant anti-inflammatory activity. Rat paw edema volume of treated animals was compared to the animals receiving ibuprofen for comparison of the relative potency. No toxic symptoms were observed after oral administration of 70 mg/Kg in the animal test.

5.3. Analgesic activity Protocol

Experimental animal

Male Swiss CD1 mice aged 4-5 weeks, average weight 25±5 g were used. They were kept under standard environmental condition for one week (relative humidity 55-65%, temperature 22 ± 2 ^{o}C and 12 h light-dark cycle) for adaptation to experimental conditions and the mice were fed with formulated rodent food and water. Mice were used only once, and were sacrificed immediately after the experiments by cervical dislocation.

Acetic acid induced writhing method[28]

Briefly, the acetic acid induced writhing method is an analgesic behavioral observation assessment method that demonstrates a noxious stimulation in mice. The test consists of injecting 25 mg/kg acetic acid solution intraperitoneally and then observing the animal for specific contraction of the body, which is referred to as ‘writhing’. A comparison of writhing

was made between positive control (NaCl solution) and the test sample which was given orally 30 min prior to acetic acid injection. If the sample possessed analgesic activity, the animal that received the sample was given a lower number of writhing than the control, i.e. the sample having analgesic activity inhibited writhing. NaCl solution was used as reference standard drug and is not analgesic.

Experimental protocol

Experimental animals were randomly selected and divided into seven groups denoted as group-CTL (NaCl), group A-1 10, group A-1 20, group A1-70, group Y-1 10, group Y-1 20 and group Y-1 70 consisting of 8 mice in each group. Each group received a particular treatment i.e. control, NaCl solution. Each mouse was weighed properly and the dose of the test samples and control materials were adjusted accordingly. Test samples and control were given orally by means of a feeding needle. A thirty minutes interval was given to ensure proper absorption of the administered substances. Then the writhing inducing chemical, acetic acid solution (0.25 mL/25 g weigh) was administered intraperitoneal to each of the animals of a group. After an interval of five minutes, which was given for absorption of acetic acid, number of squirms (writhing), 5-6 was counted for 30 minutes.

The research was carried out at the University of Barcelona, according the guide for the care and use of laboratory animals, and the experimental procedure was approved by the animal ethics committee.

5.4. Ulcerogenic Activity

Experimental animal

For the test male rat Sprague-Dawley, average weight 180±20 g was used. The mice were kept under standard environmental conditions for one week (relative humidity 55-65%, temperature

22 ± 2 ºC and 12 h light-dark cycle) for adaptation to the test environment after their purchase and fed rat formulated rodent food and water.

Experimental protocol[29]

Experimental animals were randomly selected and divided into four groups denoted as group **3**, group **5**, group **carboxymethylcellulose** and group **saline solution,** consisting of 3 rats in each group. Each group received a particular treatment i.e. control, NaCl solution. Each rat was weighed accurately and the dose of the test samples and control materials were adjusted accordingly. Test samples and control were given orally by means of a feeding needle.

Four hours after drug administration, animals were euthanized before their stomach was opened along the greater curvature, washed with saline solution and immediately the development of lesions was assessed with a magnifying glass. The quantification of gastric lesions was scored according to their number and size in a scale from 0 to 8 points (0: without injury; 1: color modification; 2: few petechial; 3: 1-3 small injuries; 4: 1-3 large injuries < 1 mm length; 5: 1-3 large injuries > 1 mm length; 6: more than three small injuries; 7: more than three large injuries and 8: more than three deep injuries.

The research was carried out on the University of Barcelona, according the guide for the care and use of laboratory animals, and the experimental procedure was approved by the animal ethics committee.

6. Molecular Modeling Methodology

6.1. Initial molecular systems for molecular modelling

The simulation protocol was based on the computational strategy used in our previous studies,[15] which is briefly summarized here. Molecular dynamics simulations were used to assess the structural integrity of the top docking poses of the studied ligands generated by RDock[30] at the

interior of the COX-2 receptor. MM-PBSA, MM-GBSA and MM-3DRISM methodologies were employed to estimate the binding free energies of the different binding modes. Three different binding modes were considered for the inhibitors according to the X-ray crystallographic structures of ibuprofen (PDB code 4PH9), diclofenac (PDB code 1PXX) and celecoxib (PDB code 3NL1) using mouse COX-2. The COX-2 enzyme receptor was built from X-ray crystallographic structure 4PH9 and used as a template for the rest of the modelling experiments. The standard protonation state at a physiological pH of 7.4 was assigned to the ionizable residues, five disulfide bonds were defined between 5-16, 6-129, 10-26, 28-38 and 539-545 residues. On the other hand, the geometry of the global minimum energy for all ligands was obtained from a systematic conformational search using the scheme B3LYP/6-31G(d)/SMD using Gaussian 09.[31] The minimum energy nature of all the stationary points was verified from the analysis of the vibrational frequencies, which were positive in all cases. The gaff force field was used to assign parameters to the inhibitors. The charge distribution of the inhibitor was further refined based on the electrostatic charges determined from a fit to the "B3LYP/6-31G(d)" electrostatic potential obtained using the RESP procedure.

6.2. Molecular dynamic simulations

All systems were initially solvated with TIP3P waters[32] in an octahedral box spanning 11 Å from the peptide to the edge of the box and neutralized with Na+ cations and additional 160 Na^+ and Cl^- ions were added to reach the 150 mM ionic strength. Approximately, a standard system comprises 1108 residues, 43.000 explicit water molecules and 166.000 atoms. All systems were subjected to minimization, thermalization and production MD simulations of a minimum duration of 60 ns for each system using AMBER14 package.[33] In some cases several replicas have been run and an extension of the MD simulation up to 120 ns has been performed (see Table 1). A multi-stage protocol was adopted for minimization and thermal equilibration of the

systems. Four minimizations (initially with 4000 cycles of steepest descent followed by a maximum of 10.000 cycles of the conjugate gradient) were run sequentially for hydrogen atoms, ions, waters and finally all atoms. Thermalization was performed in four steps in which the temperature of the system was increased from 100 to 298 K, each involving 250 ps of MD under the canonical isochoric–isothermic (NVT) ensemble, followed by MD simulation at constant temperature (298 K) and pressure (1 atm) (canonical isothermic–isobaric, NPT) lasting up to 60 ns or even 120 ns. The Amber ff14SB force field was used as implemented in the AMBER14 package[34] Langevin dynamics was employed to control the temperature, whereas Berendsen bath coupling was used for the pressure (1 atm). A time step of 2 ps was used, together with SHAKE,[35] a non-bonded cut-off of 15.0 Å, and the Particle-Mesh-Ewald (PME) method (grid spacing of 1 Å) for electrostatic interactions.

6.3. Estimation of the binding free energies

The binding free energy ($\Delta G_{binding,}$ ΔG_{bind} or ΔG_{total}) of the receptor-ligand system of both ligand sites was estimated by means of MM-PBSA, MM-GBSA and MM-3DRISM procedures using the MMPBSA.py python script as implemented in AMBER14 [36]. Both MM-PBSA and MM-GBSA methods have consistently been shown to be reliable procedures to estimate relative binding free energies for small molecules bound to protein receptors.[37] The binding process was quantified using the classical binding free energy of a reaction:

$$(1)\ \Delta G_{binding} = \Delta G_{total} = G_{complex} - G_{receptor} - G_{ligand}$$

Where $\Delta G_{binding}$ is the binding free energy, $G_{complex}$ is the free energy of the complex, $G_{receptor}$ and G_{ligand} are the free energies of the receptor and ligand, respectively. The binding free energy is the average free energy of the molecules involved in an ensemble of molecular dynamics

snapshots according to the single-trajectory method.[36] Calculations were performed for 50 snapshots taken evenly during the last 50 ns of the simulations. The ten closest waters to the ligand were also included as part of the receptor system in the calculation of the binding free energy. The reported binding free energies correspond to the average values of both equivalent binding sites in the modeled system.

The binding free energy (ΔG_{bin} or ΔG_{total}) is calculated by combining the molecular mechanical energies with the continuum solvent approaches (Poisson-Boltzmann Surface Area/PBSA and Generalized-Born Surface Area/GBSA)[38] and with the integral-equation theory of liquids (3DRISM)[39] or the solvation energies and the configurational entropy, which, after applying equation 1, can be expressed as:

$$(2)\ \Delta G_{total} = \Delta E_{MM} + \Delta G_{sol} - T\Delta S$$

Where ΔE_{MM} is the gas-phase energy expressed as the sum of the internal energy (bonds, angles and dihedrals) (ΔE_{int}), electrostatic energy (ΔE_{ele}) and van der Waals term (ΔE_{vdW}), which can be extracted directly from the molecular dynamics simulations. ΔG_{sol} accounts for the solvation energy (either of $\Delta G_{sol,PBSA}$, $\Delta G_{sol,GBSA}$ or $\Delta G_{sol,3DRISM}$), which can be decomposed into the polar and nonpolar parts (ΔG_{sol_pol} and ΔG_{sol_apol}). The configurational entropy upon complexation ($-T\Delta S$) were assumed to cancel out. Finally, the complete expression for the binding free energy is:

$$(3)\ \Delta G_{total} = \Delta E_{MM} + \Delta E_{ele} + \Delta G_{sol\_pol} + \Delta G_{sol\_apol}$$

The polar term of the solvation energy in PBSA ($\Delta G_{sol\_pol,PBSA}$) reflects the change in free energy in the transfer from the gas phase to the aqueous solvent, modelled as a homogeneous medium

and characterized by different dielectric constants. This term is calculated by applying numerical methods for solving the Poisson-Boltzmann (PB) equation through a finite-difference approach. The Poisson-Boltzmann equation depends on the interior and exterior dielectric constants and also on the ionic strength, which in this work are set to 3, 80 and 150 mM, respectively. The nonpolar contribution to the solvation energy ($\Delta G_{sol\_apol,PBSA}$) separates the non-polar solvation interactions into two terms: the repulsive (ΔG_{cav}, cavitation energy) as function of the Solvent-Accessible Surface Area (SAS) and the attractive (ΔG_{disp}, dispersion energy) interactions with the following parameters: γ = -0.5692 and β = 0.0378 kcal/mol/Å2.[40]

The GBSA model offers a simpler, computationally less-expensive approach to the electrostatic component of the solvation free energy, $\Delta G_{sol_pol,}$GBSA.[41] This function also depends on the ionic strength, which here was set to 150 mM. Here we have used a modified GB model developed and implemented by A. Onufriev, D. Bashford and D.A. Case.[42-43] Meanwhile, the nonpolar contribution ($\Delta G_{sol_apol,GBSA}$) was estimated by using a linear expression with the SAS, which is intended to account for the contributions due to the cavity formation within the solvent and the change in non-polar interactions between solute and solvent. Here, the hydrophobic contribution is approximated by the LCPO method with γ = 0.0 and β = 0.0072 kcal/mol/Å^2.[44] Other parameters in both methods not mentioned in the text were left as the default values according to the MMPBSA.py script.

Since we were interested in describing the binding mode, all the energy terms in equation 3 were decomposed into per-residue contributions according to the standard scheme:

(4) $$\Delta G_{total} = \sum_{i=1}^{n} \Delta G_i$$

Where *n* is the total number of residues, ΔGi are the per-residue contributions.[36,45] The R program[46] was used for all statistical analysis and Pymol for molecular graphics.

Acknowledgements

The Spanish Minister (CTQ2011-29285-C02-02) and SGR-(2014)-1017 Generalitat de Catalunya are gratefully acknowledged for their financial support.

Supplementary Material

Supplementary data containing complementary material of modelization studies and NMR spectra of synthesized compounds related with this article can be found, in the online version, at https://doi.org/

Conflict of interest

The authors declare no conflict of interest.

Abbreviations used

ACHN, 1,1′-azobis(cyanocyclohexane; DMDS, dimethyl sulfide; IC_{50}, inhibitory concentration at 50% inhibition; BINAP, 2,2'-*bis*(diphenylphosphino)-1,1'-binaphthyl; DCM, dichloromethane; DMF, dimethylformamide; ESI, electrospray; HMRS, high resolution mass spectrometry; NMR, nuclear magnetic resonance, PDA, protein data bank; TLC, thin layer chromatography, TFA, trifluoroacetic acid, TFAA, trifluoroacetic anhydride.

References

1. a) Bertolini A, Ottani A, Sandrini M. Selective COX-2 inhibitors and dual anti-inflammatory drugs: Critical remarks. *Curr. Med. Chem*. 2002;9:1033-1043. b) Howardell MJ. COX-2 Inhibitor Research, Editor Nova, 2006. c) Yu G, Praveen Rao PN, Chowdhury MA, Abdellatif KRA, Dong Y, Das D, Velázquez CA, Suresh MR, Knaus EE. Synthesis and biological evaluation of N-difluoromethyl-1,2-dihydropyrid-2-one acetic acid regioisomers: Dual Inhibitors of cyclooxygenases and 5-lipoxygenase. *Bioorg. Med. Chem. Lett*. 2010;20:2168-2173. d) Chowdhury MA, Abdellatif KRA, Dong Y, Das D, Suresh MR, Knaus EE. Synthesis of Celecoxib Analogues Possessing a N-Difluoromethyl-1,2-dihydropyrid-2-one 5-Lipoxygenase Pharmacophore: Biological Evaluation as Dual Inhibitors of

Cyclooxygenases and 5-Lipoxygenase with Anti-Inflammatory Activity. *J. Med. Chem*. 2009;52:1525-1529.

2. Dannhardt G, Kiefer W. Cyclooxygenase inhibitors-current status and future prospects. *Eur. J. Med. Chem*. 2001;36:109-126. b) Puig C, Crespo MI, Godessart N, Feixas J, Ibarzo J, Jiménez JM, Soca L, Cardelus I, Heredia A, Miralpeix M, Puig MJ, Beleta J, Huerta JM, López M, Segarra V, Ryder H, Palacios JM. Synthesis and Biological Evaluation of 3,4-Diaryloxazolones: A New Class of Orally Active Cyclooxygenase-2 Inhibitors. *J. Med. Chem*. 2000;43:214-223. c) Kiefer W, Dannhardt G. Novel Insights and Therapeutical Applications in the Field of Inhibitors of COX-2. *Curr. Med. Chem*. 2004;11:3147-3161.

3. Gund P, Shen TY. A model for the prostaglandin synthetase cyclooxygenase site and its inhibition by antiinflammatory arylacetic acids. *J. Med. Chem*. 1977;20:1146-1152.

4. Jouzeau JY, Terlain B, Abid A, Nedelec E, Netter P. Cyclooxigenase isoenzimes. How recent findings affect thinking about nonsteroidal anti-inflammatory drugs. *Drugs* 1997;53:563-582.

5. Moore BC, Simmons DL. COX-2 inhibition. Apoptosis and chemoprevention by nonsteroidal anti-inflammatory drugs. *Curr. Med. Chem*. 2000;7:1131-1144.

6. a) Breitner J, Baker L, Drye L, Evans D, Lyketsos C, Ryan L, Zandi P, Baker L, Breitner J, Saucedo HH, Anau J, Cholerton B, Kramer K, Bloomberg JH, Zandi P, Drye L, Shanklin Casper A, Meinert C, Martin B, Jenkins G, McCaffrey L, Meinert J, Vaidya V, Ahuja A, May P, Ryan L, Lyketsos GG, Steinberg M, Brandt J, Pedroso JJ, Bergey A, Gogel C, Smith L, Kraus J, Stern RA, Green RC, Gavett B, Mwicigi J, Baldwin L, McGowan T, Johnson P, Qiu W, Frederick J, Raghavan S, Rossi C, Mandell A, Dinizo D, Roth T, Porsteinsson A, Ismail M, Brand C, Richard J, Stear K, Schepp S, Cosman K, Martin K, Craft S, Baker L, Dahl D, Garrett G, Tidwell J, Thielke S, Smith L, Arbuckle M, Strong W, Ladenberg J, Callaghan M, Watson S, Skinner J, Bowton K, Sabbagh M, Belden C, Liebsack C, Davis K, Arnieri L, Malek-Ahmadi M, Nicholson L, Jacobson S, Schwartz E, Mullan M, Luis C, Parrish J, Faircloth M, Ervin T, Girard J, Burke D. Efficacy of naproxen, celecoxib for the prevention of Alzheimer's disease. *Alzheimers Dement* 2013;9:714-723. b) S. Lehrer S, P.H. Rheinstein PH. Is Alzheimer's Disease Autoimmune Inflammation of the Brain That Can be Treated

With Nasal Nonsteroidal Anti-Inflammatory Drugs? *Am. J. Alzheimers Dis. Other Demen*. 2015;30:225-2277.

7. a) Mc Gettigan P, Henry D. Current problems with non-specific COX inhibitors. *Curr. Pharm. Des*. 2000;6:1693-1724. b) Barbaric M, Kralj M, Marjanovic M, Husnjak I, Pavelic K, Filipavic-Grcic J, Zorc D, Zorc B. Synthesis and in vitro antitumor effect of diclofenac and fenoprofen thiolated and non-thiolated polyaspartamide-drug conjugates. *Eur. J. Med. Chem*. 2007;42:20-29. c) Badri W, Miladi K, Nazari QA, Greige-Gerges H, Fessi H, Elaissari A. Encapsulation of NSAIDs for inflammation management : Overview, progress, Challenges and prospects. *Int. J. Pharm*. 2016;515:757-773.

8. Chen L, He Y, Huang H, Liao H, Wei W. Selective COX-2 inhibitor celecoxib combined with EGFR-TKI ZD 1839 on non-small cell lung cancer cell lines: in vitro toxicity and mechanism study. *Med. Oncolog*. 2008;25:161-171.

9. a) Yao M, Zhou W, Sangha S, Albert A, Chang AJ, Liu TC, Wolfe MM. Effects of Nonselective Cyclooxygenase Inhibition with Low-Dose Ibuprofen on Tumor Growth, Angiogenesis, Metastasis, and Survival in a Mouse Model of Colorectal Cancer. *Clin. Cancer Res*. 2005;11:1618-1628. b) Thun MJ, Henley SJ, Pairono C. Nonsteroidal anti-inflammatory drugs as anticancer agents: mechanistic, pharmacologic, and clinical issues. *J. Natl. Cancer Inst*. 2002;94:252-266.

10. Soh JW, Kazi JV, Li H, Thompson WJ, Weinstein B. Celcoxib-induced growth inhibition in SW480 colon cancer cells is associated with activation of protein kinase G. *Mol. Carcinogenesis* 2008;47:519-525.

11. Harris RE, Beebe-Donk J, Doss H, Burr-Doss D. Aspirin, ibuprofen, and other non-steroidal anti-inflammatory drugs in cancer prevention: a critical review of non-selective COX-2 blockade (Review). Oncology Reports 2005;13:559-583.

12. Robak P, Smolewski P, Robak T. The role of non-steroidal anti-inflammatory drugs in the risk of development and treatment of hematologic malignances. *Leukemia&lymphoma* 2008;49:1452-1462.

13. Chen LC, Ashcroft DM. Risk of myocardial infarction Associated with selective COX-2 inhibitors: Meta-analysis of randomised controlled trials. *Pharmacoepidemiol. Drug Saf*. 2007;16:762-772.

14. Peri KG, Hardy P, Li DY, Varma DR, Chemtob S. Prostaglandin G/H Synthase-2 Is a Major Contributor of Brain Prostaglandins in the Newborn. *J. Biol. Chem*. 1995;270:24615-24620.

15. Harrak Y, Casula G, Basset J, Rosell G, Plescia S, Raffa D, Cusimano MC, Pouplana R, Pujol MD. Synthesis, Anti-inflammatory Activity and in Vitro Antitumor Effect of a Novel Class of Cyclooxigenase Inhibitors: 4-(Aryloyl)phenyl methyl sulfones. *J. Med. Chem*. 2010;53:6560-6571.

16. Navarro L, Pujol MD. Microwave assisted synthesis of selected diaryl ethers under Cu (I)-catalysis, Tetrahedron Lett. 2015;56:1812-1815.

17. Bucharan JC, Woodgate PD. The Clemmensen reduction of difunctional ketones, Q. *Rev. Chem. Soc*. 1969;23:522-536.

18. Weaver JD, Morris DK, Tunge JA. Synthesis of Chiral Nonracemic Tertiary α-Thio and α-Sulfonyl Acetic Esters via SN_2 Reactions of Tertiary Mesylates. *Synlett* 2010:470-474.

19. Uddin MJ, Rao PNP, McDonald R, Knaus EE. A new class of acyclic 2-alkyl-1,2,2-triaryl(*Z*)-olefins as selective cyclooxygenase 2 inhibitors. *J. Med. Chem.* 47 (2004;47:6108-6111.

20. Uddin MJ, Rao PNP, Knaus EE. Design and synthesis of novel celecoxib analogues as selective cyclooxygenase-2 (COX-2) inhibitors: replacement of the sulfonamide pharmacophore by a sulfonylazide bioisostere. *Bioorg. Med. Chem*. 2003;11:5273-5280.

21. Winter CA, Risley EA, Nuss GW. Carrageenin-induced edema in hind paw of rat as an assay for anti-inflammatory drugs. *Proc. Soc. Exp. Biol. Med.* 1962;111:544-547.

22. a) Wodzinski S, Bunting JW. The acidities of 4-arylsulfonylmethylpyridines and N-methyl and N-benzyl-4-arylsulfonylmethylpyridinium cations in aqueous solution. *Can. J. Chem*. 1992;70:2635-2644. b) Judka M, Wojtasiewicz A, Danikiewicz W, Makoza M. Halogens in γ-position enhance the acidity of alkyl aryl sulfones and alkane nitriles. *Tetrahedron* 2007;63:8902-8909.

23. Hall A, Atkinson S, BrownIain SH, Chessell P, Chowdhury A, Giblin GMP, Goldsmith P, Healy MP, Jandu KS, Johnson MR, Michel AD, Naylor A, Sweeting JA. Discovery of novel, non-acidic 1,5-biaryl pyrrole EP1 receptor antagonists. *Bioorg. Med. Chem. Lett*. 2007;17:1200-1205.

24. Orlando BJ, Lucido MJ, Malkowski MG. The Structure of Ibuprofen Bound to Cyclooxygenase-2, *J. Struct. Biol.* 2015;189:62-66.

25. Homeyer N, Gohlke H. Free Energy Calculations by the Molecular Mechanics Poisson-Boltzmann

Surface Area Method. *Mol. Inform.* 2012;31:114-122.

26. Gierse JK, Koboldt CM, Walker MC, Seibert K, Isakson PC. Kinetic Basis for Selective Inhibition of Cyclo-Oxygenases. *Biochem. J*. 1999:*339*-343.

27. Shamsudin Khan Y, Kazemi M, Gutiérrez-de-Terán H. Åqvist J. Origin of the Enigmatic Stepwise Tight-Binding Inhibition of Cyclooxygenase-1. *Biochemistry* 2015;54:7283–7291.

28. Dannerman PJ. In: Monitoring of analgesia in anesthesia and analgesia in laboratory animals. D.K. Kohn, K. Sally, B. Wixson B, W.J. White, G. John editors. USA: Academic Press. 1977;6:83-99.

29. Walker CL, Trevisan G, Rossato MF, Cássia R, Franciele V, Pinheiro C, Franciscato C, Etiane Tatsch D, Morett MB, Morgana D, Silva E, Manfron M, Moresco RN, Adair RS, Santos E, Pereira ME, Ferreira J. Antinociceptive activity of *Mirabilis jalapa* on acute and chronic pain models in mica, *J. Ethnopharmacol.* 2013;1489:685-693.

30. Ruiz-Carmona S, Alvarez-Garcia D, Foloppe N, Garmendia-Doval AB, Juhos S, Schmidtke P, Barril X, Hubbard RE, Morley SD. rDock: A Fast, Versatile and Open Source Program for Docking Ligands to Proteins and Nucleic Acids. *PLoS Comput. Biol.* 2014;10:e1003571.

31. Frisch MJ, Trucks GW, Schlegel HB, Scuseria GE, Robb MA, Cheeseman JR, Scalmani G, Barone V, Mennucci B, Petersson GA, Nakatsuji H, Caricato M, Li X, Hratchian HP, Izmaylov AF, Bloino J, Zheng G, Sonnenberg JL, Had M. D.J.F. Gaussian 09, Revision D.01, 2009.

32. Jorgensen WL, Chandrasekhar J, Madura JD, Impey RW, Klein ML. Comparison of Simple Potential Functions for Simulating Liquid Water. *J. Chem. Phys.* 79 (1983;79:926-935.

33.Case DA, Babin V, Berryman JT, Betz RM, Cai Q, Cerutti DS, Cheatham TE, Darden TA, Duke RE, Gohlke H, Goetz AW, Gusarov S, Homeyer N, Janowski P, Kaus J, Kolossváry I, Kovalenko A, Lee TS, LeGrand S, Luchko T, Luo R, Madej B, Merz KM, Paesani F, Roe DR, Roitberg A, Sogui C, Salomon-Ferrer R, Seabra G, Simmerling CL, Smith W, Swails J, Walker RC, Wang J, Wolf RM, Wu X, Kollman PA, AMBER 14, 2014.

34. Hornak V, Abel R, Okur A, Strockbine B, Roitberg A, Simmerling C. Comparison of Multiple Amber Force Fields and Development of Improved Protein Backbone Parameters. *Proteins* 2006;65:712-725.

35. Ryckaert JP, Ciccotti G, Berendsen HJ. Numerical Integration of the Cartesian Equations of Motion

of a System with Constraints: Molecular Dynamics of N-Alkanes. *J. Comput. Phys.* 23 (1977;23:327-341.

36. Miller BR, McGee TD, Swails JM, Homeyer N, Gohlke H, Roitberg AE. MMPBSA.py : An Efficient Program for End-State Free Energy Calculations. *J. Chem. Theory Comput.* 2012;8:3314-3321.

37. Kuhn B, Kollman PA. Binding of a Diverse Set of Ligands to Avidin and Streptavidin: An Accurate Quantitative Prediction of Their Relative Affinities by a Combination of Molecular Mechanics and Continuum Solvent Models. *J. Med. Chem.* 2000;43:3786–3791.

38. Kollman PA, Massova I, Reyes C, Kuhn B, Huo S, Chong L, Lee M, Lee T, Duan Y, Wang W. Calculating Structures and Free Energies of Complex Molecules: Combining Molecular Mechanics and Continuum Models. *Acc. Chem. Res*. 2000;33:889–897.

39. Kovalenko B. Three-Dimensional Rism Theory for Molecular Liquids and Solid-Liquid Interfaces. In *In Molecular Theory of Solvation*; Hirata, F., Ed.; Kluwer Academic: Dordrecht, the Netherlands, 2003.

40. Tan C, Tan Y.-H, Luo R. Implicit Nonpolar Solvent Models. *J. Phys. Chem. B* 2007;111:12263-12274.

41. Still WC, Tempczyk A, Hawley RC, Hendrickson T. Semianalytical Treatment of Solvation for Molecular Mechanics and Dynamics. *J. Am. Chem. Soc*. 1990;112:6127–6129.

42. Onufriev A, Bashford D, Case DA. Modification of the Generalized Born Model Suitable for Macromolecules. *J. Phys. Chem. B* 2000;104:3712-3720.

43. Onufriev A, Bashford D, Case DA. Exploring Protein Native States and Large-Scale Conformational Changes with a Modified Generalized Born Model. *Proteins* 2004;55:383-394.

44. Weiser J, Shenkin PS, Still WC. Approximate Atomic Surfaces from Linear Combinations of Pairwise Overlaps (LCPO). *J. Comput. Chem.* 1999;20:217-230.

45. H. Gohlke H, C. Kiel C, D.A. Case DA. Insights into Protein–Protein Binding by Binding Free Energy Calculation and Free Energy Decomposition for the Ras–Raf and Ras–RalGDS Complexes. *J. Mol. Biol*. 330 (2003;330:891-913.

46. Team, RCR. A Language and Environment for Statistical Computing**, 2012.**

Graphical Abstract:

Synthesis and biological properties of aryl methyl sulfones

Lorena Navarro, Gloria Rosell, Silvia Sánchez, Núria Boixareu, Klaus Pors, Ramon Pouplana, Josep M. Campanera, and M. Dolors Pujol

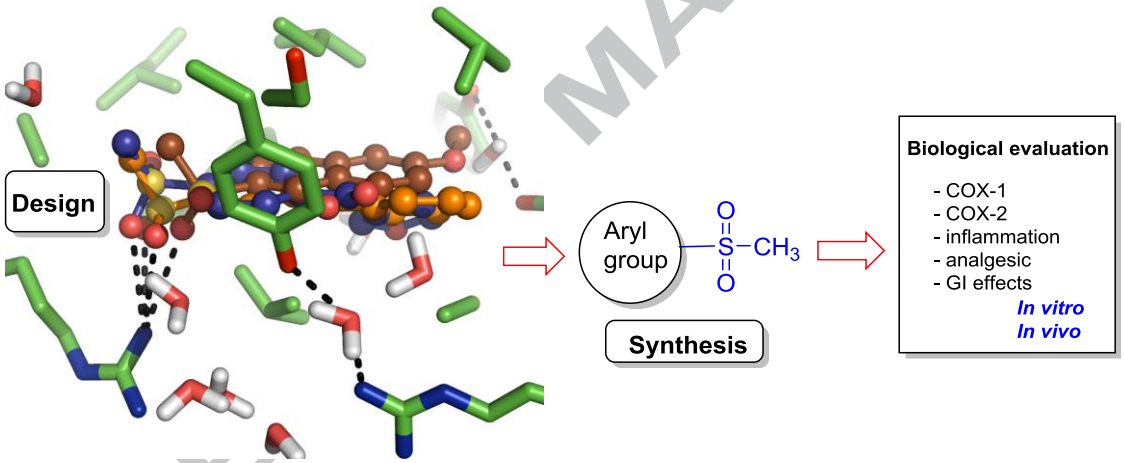

Highlights

- Aryl methyl sulfones related to classical AINEs were designed and synthesized
- Anti-inflammatory activity was evaluated in classical assays in vivo and in vitro
- The rigid compounds showed better activity than the more flexible ones
- **2** and **7** are promising compounds for the treatment of inflammatory processes
- The methyl sulfones did not show GI effects